

Optimal transport weights for causal inference

Eric A. Dunipace^{*1,2}

¹Department of Biostatistics, Harvard T.H. Chan School of Public Health

²David Geffen School of Medicine at UCLA

Abstract

Weighting methods are a common tool to de-bias estimates of causal effects. And though there are an increasing number of seemingly disparate methods, many of them can be folded into one unifying regime: Causal Optimal Transport. This new method directly targets distributional balance by minimizing optimal transport distances between treatment and control groups or, more generally, between a source and target population. Our approach is semiparametrically efficient and model-free but can also incorporate moments or any other important functions of covariates that the researcher desires to balance. We find that Causal Optimal Transport outperforms competitor methods when both the propensity score and outcome models are misspecified, indicating it is a robust alternative to common weighting methods. Finally, we demonstrate the utility of our method in an external control study examining the effect of misoprostol versus oxytocin for the treatment of post-partum hemorrhage.

1 Introduction

1.1 Weighting in causal inference

Weighting is a versatile methodology used in a variety of fields. In survey sampling, weighting can adjust for unit-level non-response to give unbiased estimates of sample means; in causal inference, weighting can adjust for unit-level treatment decisions to give unbiased estimates of causal effects. Most weighting methods in causal inference explicitly or implicitly model the treatment assignment mechanism and generate a propensity score, or an individual's probability of having received treatment (Rosenbaum and Rubin, 1983). Inverse propensity score weighting (IPW) weights observations by the inverse of these treatment probabilities to yield estimates of treatment effects (Rosenbaum, 1987; Robins et al., 1994; Rotnitzky et al., 1998).

^{*}edunipace@mail.harvard.edu

The mechanism by which IPW works is simple: it weights the distribution in a source sample to look like the distribution in some target sample of interest. For example, the source sample could be the controls who we wished looked more like the treated.

However, typical models for IPW estimators are not without their problems. One potential issue is that the propensity score model must be correctly specified—or at least offer predictions close to the correct specification—to get good estimates of causal effects. Additionally, estimators based on the propensity score can become unstable when the estimated propensity scores are close to 0 or 1 (Kang and Schafer, 2007).

1.2 Weighting for covariate balance

Other weighting methods address these concerns by instead balancing observable functions of the covariates so that performance can be empirically assessed (Imai and Ratkovic, 2014; Hainmueller, 2012; Zubizarreta, 2012). These methods will perform well when the chosen covariate functions either lead to the balance of the distributions or to balance of the basis functions that determine the conditional mean outcome given the covariates (Fan et al., 2016; Ratkovic and Tingley, 2017; Wang and Zubizarreta, 2019a; Li and Li, 2021). Though these basis functions are rarely known in practice, applied researchers are often able to specify outcome models that in turn suggest hypothesized basis functions. Additionally, sieve estimation can address this issue by expanding the set of basis functions with the sample size.

Other authors use more directly non-parametric approaches through reproducing Kernel Hilbert spaces (RKHS), which in principle capture the basis functions of the data but require the estimation of unknown tuning parameters (Kallus, 2016; Kallus et al., 2018; Wong and Chan, 2018; Kallus and Santacatterina, 2019). However, even these models still fail to capture something critical about the covariates: the joint distribution.

1.3 The central role of distributional balance in causal inference

Ultimately, a lack of distributional balance between groups leads to biased estimates of causal effects. If the distributions are the same between source and target samples, then all basis functions that determine the conditional mean function will also be balanced and treatment effect estimates will be unbiased (Figure 1).

Of course, balancing the correct basis functions is sufficient to estimate unbiased treatment effects. But when these basis functions are misspecified, methods directly targeting distributional balance can potentially perform better. Fortunately, we do not have to choose between basis function or distributional balance—we can do both.

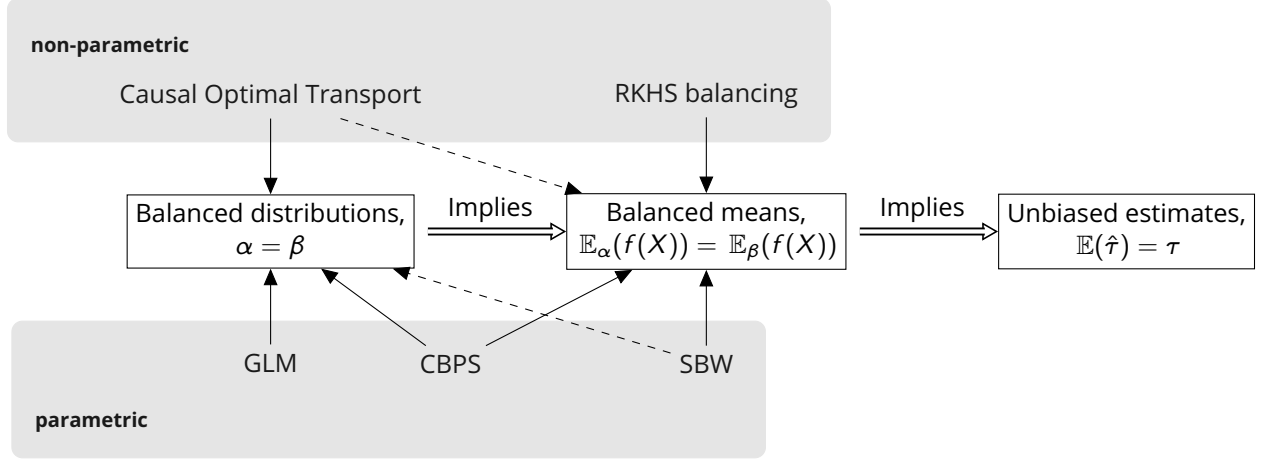


Figure 1: Different methods and their target for balance. α and β are two arbitrary distributions between groups, X is the vector of covariates, and τ is the treatment effect. RKHS = reproducing kernel Hilbert space, GLM = generalized-linear-model-based IPW, CBPS = covariate balancing propensity score (Imai and Ratkovic, 2014), and SBW = stable balancing weights (Zubizarreta, 2015). Dotted lines indicate the potential of these methods to perform the highlighted task. If the targeted basis functions actually determine the propensity score, then RKHS and SBW will also likely balance the distributions as well.

1.4 Causal optimal transport

We propose a new method that achieves distributional and basis function balance in one framework: Causal Optimal Transport. As we document, our method performs well compared to competitor weighting methods in simulation studies—especially when the propensity score and outcome models are misspecified. Moreover, our weights obtain the semiparametric efficiency bound. We also demonstrate that several methods in the literature such as synthetic control methods and nearest neighbor matching with replacement are actually special cases of Causal Optimal Transport. Thus, our framework can be seen as an interpolation of many methods that seek distributional balance.

We proceed as follows: in Section 2, we describe the setting and assumptions necessary for identification. Then we discuss the relevant features of Causal Optimal Transport such as the specific problem formulation, practical considerations for using the method, and statistical inference in Section 3. In Section 4, we demonstrate how causal optimal transport unifies many existing methods in the literature, and in Section 5, we provide simulation results demonstrating the utility of our method. Section 6 presents a case study utilizing our method on an observational study created from a multi-site randomized control trial (RCT) studying post-partum hemorrhage. Finally, we offer our concluding remarks in Section 7.

2 Setup

2.1 The potential outcomes framework

We adopt the potential outcomes framework of Neyman and Rubin (Splawa-Neyman, 1923; Rubin, 1974). Assume that we have an independent, identically distributed (iid) sample of $n \in \mathbb{N}$ units from some population. Let Z be a binary variable that denotes receiving a treatment ($Z = 1$) or control ($Z = 0$) condition. $Y(0)$ and $Y(1)$ denote the potential outcomes, only one of which is observed. Then we denote the observed outcome as $Y = Z \cdot Y(1) + (1 - Z) \cdot Y(0)$, which is defined on a space $\mathcal{Y} \subseteq \mathbb{R}$, and the confounders as $X \in \mathcal{X} \subseteq \mathbb{R}^d$. We will assume we have $n_0 \in \mathbb{N}$ control units and $n_1 \in \mathbb{N}$ treated units giving $n = n_0 + n_1$ total observations from this sample.

Suppose we also have a second sample of $m \in \mathbb{N}$ units drawn iid from a potentially different population. We also measure covariates $X \in \mathcal{X}$, but the outcome Y and treatment indicator Z are not observed. Our goal is then to use the information in the first set of samples, the **source**, to make inferences about the second set of samples, the **target**. Let $S = 1$ if an observation is in the source sample and $S = 0$ if an observation is in the target sample.

To avoid confusion, we will let $i \in \{1, \dots, n\}$ index units in the source sample and $j \in \{n+1, \dots, n+m\}$ index units in the target sample. Further, denote the empirical distribution of the source sample as $\mathbf{a} = \sum_i \delta_{x_i} a_i$ and the empirical distribution in the target sample as $\mathbf{b} = \sum_j \delta_{x_j} b_j$. We will denote their population level counterparts as α and β , respectively. Since \mathbf{a} and \mathbf{b} are iid, their empirical masses will be equal to the reciprocal of the sample size, *i.e.* $a_i = 1/n$ and $b_j = 1/m$, but this does not have to be the case. The empirical distribution in the treated group of the source sample will be defined as $\mathbf{a}_1 = \frac{1}{n_1} \sum_i \delta_{x_i} Z_i$ and the empirical distribution in the control group of the source sample will be defined as $\mathbf{a}_0 = \frac{1}{n_0} \sum_i \delta_{x_i} (1 - Z_i)$.

Finally, we assume the space \mathcal{X} has a distance metric between observations, $d_{\mathcal{X}}(x_i, x_j) \in \mathbb{R}_+$. We will define a generic cost function as $c(x_i, x_j) = d_{\mathcal{X}}(x_i, x_j)^p$ with $p \geq 1$. This could be any number of well known functions. For example, if $d_{\mathcal{X}}$ is the Euclidean distance and $p = 2$, then c is the squared-Euclidean distance. From this function, we then construct a pairwise cost matrix $\mathbf{C} \in \mathbb{R}_+^{n \times m}$ between each unit i and j : $\mathbf{C}_{ij} = c(x_i, x_j)$.

2.2 Causal estimands

There are several potential causal contrasts of interest over these populations. The first is of the form

$$\tau_{\text{sate}} = \mathbb{E}_{\alpha} \{Y(1) - Y(0)\}, \quad (1)$$

or the average treatment effect in the source population (SATE) and the second is of the form

$$\tau_{\text{tate}} = \mathbb{E}_{\beta} \{Y(1) - Y(0)\}, \quad (2)$$

or the average treatment effect in the target population (TATE). However, we cannot estimate (2) since both potential outcomes are completely missing.

Instead, we need to use the information in the source population to get valid estimates of treatment effects. That is, we desire

$$\mathbb{E}_{\alpha} \{Y(z) \cdot w\} = \mathbb{E}_{\beta} \{Y(z)\},$$

for some function w . A common way to do this is to use an importance sampling weight where $w = \frac{d\beta}{d\alpha}$, also known as the Radon-Nikodym derivative of β with respect to α . In effect, we make the distributions the same to make the expectations the same. This is the idea behind using the propensity score in IPW. An alternative strategy is to find a w such that the integrals are equal but not necessarily such that the densities are themselves the same. This is the idea behind basis function balancing.

In either case, we estimate (2) as

$$\hat{\tau}_{\text{tate}} = \sum_i w_i Y_i Z_i - \sum_i w_i Y_i (1 - Z_i), \quad (3)$$

with the constraint that the weights sum to 1 in the treatment and control groups of the source sample: $\sum_i w_i Z_i = \sum_i w_i (1 - Z_i) = 1$.

2.3 Identifying assumptions

To identify these estimators, we need several assumptions, which we formalize below.

Assumption 1

Stable unit treatment value assumption, (Rubin, 1986)

(i) *No interference between units:*

$$Y_i(Z_1, Z_2, \dots, Z_i, \dots, Z_n) = Y_i(Z_i)$$

(ii) *No hidden versions of treatments:*

$$Y_i(Z_i) = Y_i(z) \text{ if } Z_i = z.$$

Assumption 2

Strong ignorability of treatment assignment, (Rosenbaum and Rubin, 1983)

$$(i) Y(0), Y(1) \perp\!\!\!\perp Z \mid X, S = 1$$

$$(ii) 0 < P(Z = 1 \mid X, S = 1) < 1.$$

Assumption 3

Strong ignorability of sampling

$$(i) Y(0), Y(1) \perp\!\!\!\perp S \mid X$$

$$(ii) 0 < P(S = 1 \mid X) < 1$$

Assumption 1 ensures that units do not interfere with each other and that we can use the observed outcomes to estimate our causal effects. Assumption 2 (i) is the unconfoundedness assumption and (ii) ensures the distributions of the controls and treated in the source population overlap, at least asymptotically. Lastly, Assumption 3 (i) ensures the unconfoundedness of the sampling indicator with the potential outcomes and (ii) requires that the distributions of α and β are defined over the same space with both putting positive mass on the same sets. This is a slightly stronger assumption than is strictly necessary since we only require that $\beta \ll \alpha$, i.e. $\alpha(E) = 0 \Rightarrow \beta(E) = 0$ for every measurable set E .

Before we discuss our weighting method for distributional balance, we introduce optimal transport and share some properties that will be useful for our later discussion.

3 Causal Optimal Transport

3.1 Properties of optimal transport

The popularity of optimal transport methods have exploded in recent years thanks to several theoretical and methodological advances in a variety of fields. This section will serve as a brief introduction for the uninitiated explaining some of the relevant concepts and results. For a longer treatment, see the book by Peyré and Cuturi (2019).

The original optimal transport problem formulated by Monge (1781) involves finding optimal maps between distributions. Define such a map as a function $T : \mathcal{X} \mapsto \mathcal{X}$ and such that $\int_{\mathcal{X}} g(x) d\alpha = \int_{\mathcal{X}} g(T(x)) d\beta$ for all measurable functions g . We denote the corresponding push-forward operator from β to α as $T_{\#}\beta = \alpha$. The Monge (1781) formulation of the optimal transport problem is then

$$\inf_T \int_{\mathcal{X}} c(T(x), x) d\beta, \tag{4}$$

where $T_{\#}\beta = \alpha$. Unfortunately, this problem can be intractable to solve in practice.

To alleviate this issue, the Kantorovich (1942) formulation instead considers probabilistic assignments between distributions α and β :

$$\text{OT}(\alpha, \beta) = \min_{\pi \in \Pi(\alpha, \beta)} \int_{\mathcal{X} \times \mathcal{X}} c(x, x') d\pi(x, x'), \quad (5)$$

where $\Pi(\alpha, \beta)$ is the set of probability distributions over $\mathcal{X} \times \mathcal{X}$ with margins α and β . This metric is a proper distance that obeys the triangle inequality and metrizes the convergence in distribution, *i.e.* $\text{OT}(\alpha, \beta) = 0 \iff \alpha = \beta$ (Proposition 2.3, Peyré and Cuturi, 2019). When $c(x, x') = d_{\mathcal{X}}(x, x')^p$, as is the case for our setting, then Eq. (5) is also known as the p -Wasserstein distance.

In finite samples, the problem in Eq. (5) is a linear program that specifies the minimal cost of moving mass between empirical measures \mathbf{a} and \mathbf{b} :

$$\text{OT}(\mathbf{a}, \mathbf{b}) = \min_{\mathbf{P} \in \mathbf{U}(\mathbf{a}, \mathbf{b})} \sum_{i,j} \mathbf{C}_{ij} \mathbf{P}_{ij} \quad (6)$$

where $\mathbf{U}(\mathbf{a}, \mathbf{b})$ is the set of measures with margins \mathbf{a} and \mathbf{b} . The entries of \mathbf{P} form probabilistic matches between source and target samples and are akin to relaxed versions of optimal matching (Rosenbaum, 1989). Unfortunately, this problem is known to have a decaying convergence with increasing dimension (Fournier and Guillin, 2015; Weed and Bach, 2017) and also to suffer from a large computational complexity (Solomon et al., 2015).

Fortunately, regularized optimal transport offers improved rates of convergence (Genevay et al., 2018b; Mena and Weed, 2019) and computational speed (Altschuler et al., 2017; Blondel et al., 2018) by adding a convex penalty to the objective function:

$$\text{OT}_{\lambda}(\mathbf{a}, \mathbf{b}) = \min_{\mathbf{P} \in \mathbf{U}(\mathbf{a}, \mathbf{b})} \sum_{i,j} \mathbf{C}_{ij} \mathbf{P}_{ij} + H_{\lambda}(\mathbf{P}_{ij}). \quad (7)$$

Common penalties for H_{λ} include an entropy penalty, $\lambda \mathbf{P}_{ij} \log \mathbf{P}_{ij}$ (Cuturi, 2013), or an L_2 penalty, $\frac{\lambda}{2} \mathbf{P}_{ij}^2$ (Blondel et al., 2018). The solutions to this problem converge to the solutions from Eq. (6) as $\lambda \rightarrow 0$, while as $\lambda \rightarrow \infty$, the solutions put equal weight on every entry in \mathbf{P} .

To adjust for the fact that $\text{OT}_{\lambda}(\mathbf{a}, \mathbf{b}) \neq 0$, Genevay et al. (2018a) introduce the Sinkhorn divergence for entropy penalized optimal transport:

$$S_{\lambda}(\mathbf{a}, \mathbf{b}) = \text{OT}_{\lambda}(\mathbf{a}, \mathbf{b}) - \frac{1}{2} \text{OT}_{\lambda}(\mathbf{a}, \mathbf{a}) - \frac{1}{2} \text{OT}_{\lambda}(\mathbf{b}, \mathbf{b}).$$

This has the advantage that $S_\lambda(\mathbf{a}, \mathbf{a}) = 0 \iff \mathbf{a} = \mathbf{b}$ (Feydy et al., 2018), while retaining the computational and theoretical advantages of regularized optimal transport.

Finally, we can use the transportation plans found in Eqs. (6) or (7) to construct a Monge map as in Eq. (4) known as the barycentric projection or Brenier map (Ambrosio et al., 2005). In finite samples, this function can be estimated from the Kantorovich formulation as

$$T_{\mathbf{b} \rightarrow \mathbf{a}}(X_j) = \operatorname{argmin}_v \sum_i c(X_i, v) \mathbf{P}_{ij}. \quad (8)$$

For the squared-Euclidean cost, this map equals $\frac{1}{b_j} \sum_i \mathbf{P}_{ij} X_i$, or the weighted mean of the observations in the source sample. For an L_1 cost, $T_{\mathbf{b} \rightarrow \mathbf{a}}$ is the weighted median of the X_i .

3.2 Problem formulation

We define the Causal Optimal Transport problem as either

$$\text{COT}_\lambda(\mathbf{b}) = \min_{\mathbf{w} \in \Delta_n} \text{OT}_\lambda(\mathbf{w}_1, \mathbf{b}) + \text{OT}_\lambda(\mathbf{w}_0, \mathbf{b}) \quad (9)$$

or

$$\text{COT}_\lambda(\mathbf{b}) = \min_{\mathbf{w} \in \Delta_n} S_\lambda(\mathbf{w}_1, \mathbf{b}) + S_\lambda(\mathbf{w}_0, \mathbf{b}), \quad (10)$$

where \mathbf{w}_z is the empirical measure $\sum_i \delta_{x_i} w_i \mathbb{I}(Z_i = z)$ and Δ_n is the simplex with n vertices. The Causal Optimal Transport weights will then be the weights that minimize $\text{COT}_\lambda(\mathbf{b})$. In a slight abuse of notation, we have:

$$\mathbf{w}_{\text{COT}} = \operatorname{argmin}_{\mathbf{w} \in \Delta_n} \text{COT}_\lambda(\mathbf{b}). \quad (11)$$

One advantage of the formulation in Eq. (9) is that it allows for the estimation of probabilistic assignments between units, the transport matrix \mathbf{P}_{COT} , which can then be used to construct barycentric projections as in Eq. (8). However, one can construct the transport matrix *a posteriori* for Eq. (10) by solving $\text{OT}_{\lambda'}(\mathbf{w}_{\text{COT}}, \mathbf{b})$, for any $\lambda' \geq 0$. The barycentric projection can then impute the missing potential outcomes: $\hat{Y}_j(z) = \operatorname{argmin}_v \sum_i \mathbb{I}(Z_i = z) c(Y_i, v) \mathbf{P}_{ij}$.

In addition, a researcher may also know a set of functions that he or she thinks are important to balance *a priori* for valid causal estimates. These functions may include a hypothesized outcome model or the moments of the covariates. Define $B_k(\cdot) : \mathcal{X} \mapsto \mathbb{R}$ for $k \in \{1, \dots, K\}$ as these K functions of interest. Then

we can add an additional constraint to the problems in Eqs. (9) and (10) to approximately balance these functions between samples:

$$\left| \sum_{i: Z_i=z} B_k(X_i) w_i - \frac{1}{m} \sum_j B_k(X_j) \right| \leq \delta_k, \forall k \in \{1, \dots, K\}. \quad (12)$$

If these functions are well-chosen, they should improve the performance of the subsequent weighting estimators and improved rates of convergence (Wang and Zubizarreta, 2019b).

3.3 Convergence

We now discuss the convergence of our weights to the distribution of interest. First, we define the importance sampling weights as $\check{w}_i^* = \frac{d\beta(X_i)}{d\alpha(X_i)}$ and define the self-normalized importance sampling weights as $\mathbf{w}_i^* = \frac{\check{w}_i^*}{\sum_i \check{w}_i^*}$. In our setting targeting the TATE, $\check{w}_i^* = \mathbb{P}(S = 0 | X_i) / \{\mathbb{P}(Z_i = z | X_i, S_i = 1) \mathbb{P}(S = 1 | X_i)\}$. Further, let δ_n be the smallest value of the balancing function constraints at which the importance sampling weights satisfy condition (12) for sample size n . Then we rely on a few additional assumptions to prove the convergence of the Causal Optimal Transport weights.

Assumption 4

Assumptions for convergence:

4.1: $\exists x_0 \in \mathcal{X} : \int_{\mathcal{X}} c(x_0, x') d\beta < \infty$

4.2: For $\text{COT}_\lambda(\mathbf{b})$ in Eq (9) with an entropy penalty: $\lambda \rightarrow 0$ as $n \rightarrow \infty$

4.3: For the balancing of basis functions: $\mathbb{E}_\beta |B(X)| < \infty$ and $\|\delta_n\|^2 = o_p(\|\delta\|^2)$

Assumption 4.1 simply requires that the expected cost is finite while Assumption 4.2 is necessary for the convergence of the entropy penalized Causal Optimal Transport weights that do not use the Sinkhorn divergence. Assumption 4.3 requires that the expectation of the balancing functions be finite and that there is a sample size at which the importance sampling weights satisfy the balancing function constraints of Eq. (12).

With these assumptions, each version of the Causal Optimal Transport weights converges to the distribution β .

Theorem 1

If Assumptions 2–4 hold, then as $n, m \rightarrow \infty$,

$$\mathbf{w}_{\text{COT}} \rightarrow \beta,$$

where \mathbf{w}_{COT} is defined in Eq. (11).

This also means that the Causal Optimal Transport weights converge to inverse of the propensity score.

Corollary 1

As $n, m \rightarrow \infty$,

$$\lim_{n, m \rightarrow \infty} \mathbf{w}_{COT} = \lim_{n, m \rightarrow \infty} \mathbf{w}^*.$$

This follows as a consequence of the Radon-Nikodym theorem.

We are also interested in the speed at which the Causal Optimal Transport weights converge, but we need some additional assumptions.

Assumption 5

Assumptions for \sqrt{n} -bounds:

5.1 : $c(\cdot, \cdot)$ is in \mathcal{C}^∞ and is L -Lipschitz

5.2 : For entropy penalized weights, either:

$$\frac{1}{\lambda^{(5d/4)+2}} \frac{1}{\sqrt{n}} = o_p(1) \text{ and } \alpha \text{ and } \beta \text{ are } \sigma^2\text{-subgaussian with } c = \|\cdot\|_2^2$$

or:

$$\frac{\exp(\|\mathbf{C}\|_\infty/\lambda)}{\lambda^{[d/2]}} \frac{1}{\sqrt{n}} = o_p(1) \text{ and } \mathcal{X} \subset \mathbb{R}^d$$

5.3 : For L_2 penalized weights, $c(\cdot, \cdot) = d_{\mathcal{X}}(\cdot, \cdot)^p$, with $p > d/2$ and $\mathbb{E}|X|^q < \infty$ for $q > 2p$

Assumption 5.1 forces smoothness onto the cost function, and Assumption 5.2 requires a few things. First, it requires that the penalty not decrease to 0 too quickly. It further assumes that either the cost function is the squared-Euclidean distance and α, β are subgaussian or that α, β are defined on a subset of \mathbb{R}^d . Finally, Assumption 5.3 places a requirement on the cost function to be a distance metric raised to a power that is more than half the number of covariates, $d/2$, and with a distribution that has enough finite moments. These assumptions give us our next theorem.

Theorem 2

If Assumptions 2-5 hold, then

$$\mathbb{E}\{\text{OT}_\lambda(\mathbf{w}_{COT}, \mathbf{b}) - \text{OT}_\lambda(\beta, \beta)\} = \mathcal{O}\left(\frac{1}{\sqrt{n}}\right).$$

Proofs of these theorems and the corollary are provided in Appendices A and B. For a demonstration of the \sqrt{n} -convergence of the Causal Optimal Transport weights, see Appendix A.2.

3.4 Statistical Inference

For statistical inference, we turn our attention to the asymptotic distribution of Eq. (3) and its variance. Before introducing our theorem, we require some additional assumptions.

Assumption 6

Assume the following conditions hold:

$$\mathbf{6.1}: \mathbb{E}|Y - \mu_z(X)| < \infty \text{ for } \mu_z(X) \stackrel{\text{def.}}{=} \mathbb{E}(Y(z) | X)$$

$$\mathbf{6.2}: \mathbb{E}(Y^2) < \infty$$

$$\mathbf{6.3}: S_\lambda(\mathbf{w}_{\text{COT}}, \mathbf{b}) = o_p(n^{-1/2}) \text{ or for basis function balancing } \|\delta\|_2^2 = o_p(n^{-1/2}) \text{ and } \mu_z(X) \subseteq B(X)^\top \gamma, \text{ for } \gamma \in R^K$$

The first part of Assumption 6 enforces integrability of the residual. Assumption 6.2 enforces a finite second moment on the outcome so that a variance exists. Finally, Assumption 6.3 states that the Causal Optimal Transport weights are able to approximate the empirical distribution or the basis functions in finite samples more quickly than the asymptotic quantities.

With this, we have our next theorem.

Theorem 3

If Assumptions 1–6 hold, then as $n, m \rightarrow \infty$,

$$\sqrt{n}(\hat{\tau}_{\text{tate}} - \tau_{\text{tate}}) \xrightarrow{\mathcal{L}} \mathcal{N}(0, V_{\text{opt}}),$$

where V_{opt} is the semiparametrically efficient variance as in Theorem 1 of Hahn (1998).

This result follows from the fact that the bias $\hat{\tau}_{\text{tate}} - \tau_{\text{tate}}$ has the form of the semiparametrically efficient score function and that the weights converge at a \sqrt{n} -rate. For a proof of this theorem and an empirical examination of confidence interval coverage, see Appendix C. Of note, the Causal Optimal Transport weights are semiparametrically efficient without any need for model augmentation.

3.5 Practical considerations

In this section, we turn to the practical considerations of optimizing the Causal Optimal Transport weights. Namely, we discuss the tuning of the hyperparameters and estimation of the weights.

Algorithm 1: Choosing hyperparameters for the optimal transport weights

Data: Grid of parameter values $\Delta = \{\{\lambda_1, \delta_1\}, \{\lambda_2, \delta_2\}, \dots\}$, number of bootstrap samples K , empirical measure \mathbf{b} , empirical measure \mathbf{a} , treatment group of interest z , $\lambda' \geq 0$

Result: Value of hyperparameters, $\hat{\lambda}, \hat{\delta}$

foreach $\{\lambda, \delta\} \in \Delta$ **do**

 Estimate weights \mathbf{w}_{COT} given parameters $\{\lambda, \delta\}$;

for k in $1, \dots, K$ **do**

 Bootstrap new target data $\mathbf{b}_k^* \sim \mathbf{b}$;

 Bootstrap new source data $\mathbf{a}_k^* \sim \mathbf{a}$;

 Set the unnormalized weights for empirical measure in treatment group z as

$\tilde{\mathbf{w}}_k^* = \mathbf{Z} \odot \mathbf{w} \odot \mathbf{a}_k^*$, where \odot is the element-wise product ;

 Renormalize the weights, $\mathbf{w}_k^* = \tilde{\mathbf{w}}_k^* / (\tilde{\mathbf{w}}_k^{*\top} \mathbf{1}_n)$;

 Set $T_{\{\lambda, \delta\}} = K^{-1} \sum_k \text{OT}_{\lambda'}(\mathbf{w}_k^*, \mathbf{b}_k^*)$

return $\hat{\lambda}, \hat{\delta} = \text{argmin}_{\{\lambda, \delta\}} T_{\{\lambda, \delta\}}$;

Hyperparameter tuning. Our goal is to select the hyperparameters λ and δ so that we achieve the best distributional balance without overfitting the current data. To do so, we propose a bootstrap based tuning procedure detailed in Algorithm 1.

We justify this procedure in two ways. First, while practitioners may have subject matter knowledge about the degree of desired balance in the basis functions or the selection of covariates, they probably do not have an ideal weight penalty in mind. Second, because the minimum weights target the Radon-Nikodym derivative, we can use this fact to justify a bootstrap-based algorithm to select the hyperparameters that provide the best out of sample balance.

Weight estimation. Given the known complexity of estimating optimal transport distances, Huling and Mak (2020) raise the concern that using this methodology will not be feasible. Fortunately, these concerns are addressed by using regularized optimal transport. Regularized optimal transport problems are convex optimization programs (Cuturi, 2013; Blondel et al., 2018; Feydy et al., 2018) and enjoy improved computational complexity (Altschuler et al., 2017; Dvurechensky et al., 2018).

In our simulations, we find that estimating the Causal Optimal Transport weights only takes a few seconds for a 1000 observations. Eq. (9) can be optimized using LBFGS solvers from Pytorch (Paszke et al., 2019) or `lbfgsb3c` in R (Fidler et al., 2020), or in software such as the Mosek optimization suite (MOSEK ApS, 2021). Eq. (10) can be solved by alternating Sinkhorn divergence calculations in GeomLoss (Feydy et al., 2018) with optimization steps on the weights: with balancing constraints, we use the Frank-Wolfe algorithm (Frank and Wolfe, 1956); without balancing constraints, we can use an LBFGS algorithm.

3.6 Multi-valued treatments

Finally, Causal Optimal Transport is easily extended to more than two treatments as long as the treatment values are discrete. This is because we estimate the weights separately for each treatment group in the source population.

4 Connections to existing methods

The Causal Optimal Transport framework is actually related to several other methods in the literature as discussed below.

4.1 Synthetic control method

Abadie and Gardeazabal (2003) first proposed the synthetic control method (SCM) as a way of performing counterfactual inference for a single treated unit, j . The objective function is

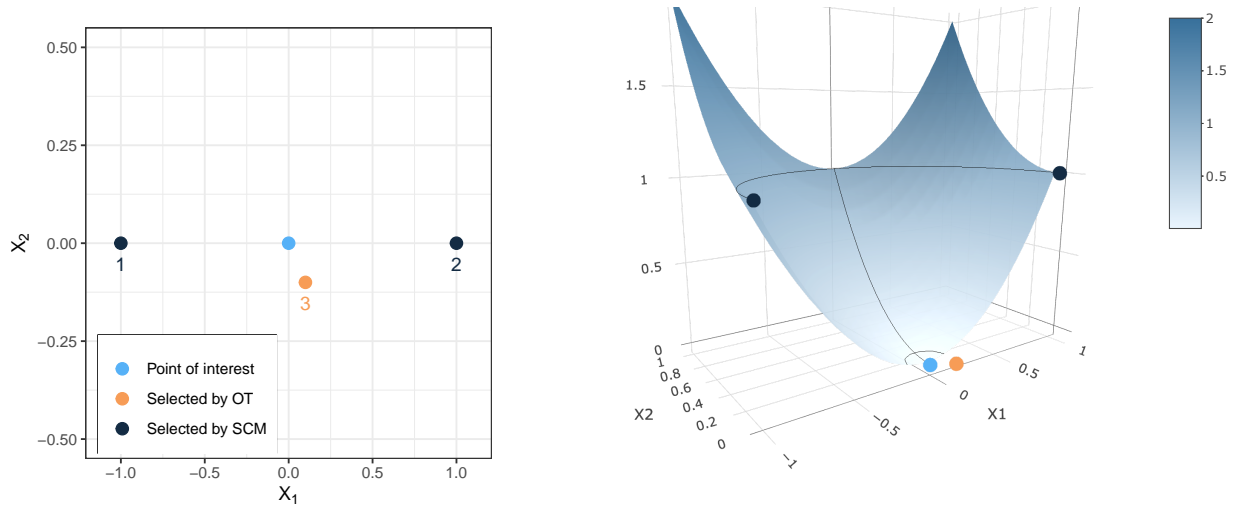
$$\min_{w: w^T \mathbf{1}_n = 1, w_i \geq 0} \left\| \sum_i X_i w_i - X_j \right\|_2^2,$$

which is the same as the Monge map in Eq. (4) when c is the squared Euclidean distance and T has the corresponding form of the barycentric projection in Eq. (8). This means that SCM is estimating a barycentric projection and is a version of the Causal Optimal Transport problem.

One potential drawback of using SCM versus the Kantorovich formulation of Causal Optimal Transport can be seen in the following simple example in Figure 2. Causal Optimal Transport favors the nearest point while the SCM method utilizes the points further away, which could be a problem if the response surface looks like Figure 2b. To avoid this, SCM could incorporate a modified objective that directly models both the barycentric projection and distance between units as in Perrot et al. (2016).

4.2 Optimal matching

The optimal matching framework of Rosenbaum (1989) is closely related to Causal Optimal Transport. Rosenbaum formulates his method as a network flow problem that seeks to minimize the overall distance between matched pairs and optimal transport can be formulated as a network flow problem. Optimal



(a) Potential points for selection and the point of interest. (b) A response surface where synthetic controls would lead to poor estimates.

Figure 2: A simple example where synthetic controls (SCM) would perform worse than Causal Optimal Transport.

matching corresponds to Causal Optimal Transport weights with integer solutions and $\lambda = 0$:

$$\begin{aligned} & \min_{\mathbf{P} \in \{0,1\}} \sum_{i,j} \mathbf{C}_{ij} \mathbf{P}_{ij} \\ & \text{subject to } \sum_i \mathbf{P}_{ij} \mathbb{I}(Z_i = z) = 1, \forall j. \end{aligned}$$

4.3 Nearest neighbor matching

When done with replacement, nearest neighbor matching is simply a re-formulation of the Causal Optimal Transport problem with $\lambda = 0$. Doing so gives the following objective:

$$\begin{aligned} & \min_{\mathbf{P} \geq 0} \sum_{i,j} \mathbf{C}_{ij} \mathbf{P}_{ij} \\ & \text{subject to } \sum_{i,j} \mathbf{P}_{ij} \mathbb{I}(Z_i = z) = 1 \\ & \mathbf{P}^\top \mathbf{1}_n = \mathbf{b}. \end{aligned}$$

This will seek to find the unit i that is closest in terms of \mathbf{C} for each unit j , which is the definition of nearest neighbor matching with replacement.

4.4 MIP matching

Mixed integer programming (MIP) matching seeks to match units to satisfy some balance criteria such as the mean or any other desired basis function, in addition to distributional balance (Zubizarreta, 2012). We can formulate the MIP objective similar to Causal Optimal Transport:

$$\begin{aligned}
& \min_{\mathbf{P} \in \{0,1\}} \sum_{i,j} \mathbf{C}_{ij} \mathbf{P}_{ij} \\
& \text{subject to } \mathbf{P}^\top \mathbf{1}_n = \mathbf{1}_m \\
& \mathbf{P} \mathbf{1}_m = L \mathbf{1}_n \\
& \left| \sum_{i,j} \frac{B_k(X_i) \mathbf{P}_{ij}}{Lm} - \frac{1}{m} \sum_j B_k(X_j) \right| \leq \delta_k, \quad \forall k \in \{1, \dots, K\},
\end{aligned}$$

for $L \geq 1$. Like optimal matching, this is similar to the formulation of the full Causal Optimal Transport objective but with integer weights.

4.5 Energy distance and the MMD

The energy distance is defined as

$$\mathcal{E}(\mathbf{a}, \mathbf{b}) = \frac{2}{nm} \sum_{i,j} d_{\mathcal{X}}(x_i, x'_j)^p - \frac{1}{n^2} d_{\mathcal{X}}(x_i, x_i)^p - \frac{1}{m^2} d_{\mathcal{X}}(x'_j, x'_j)^p,$$

where $p \geq 1$ (Feydy et al., 2018). Then $S_\lambda(\mathbf{a}, \mathbf{b}) \rightarrow \frac{1}{2} \mathcal{E}(\mathbf{a}, \mathbf{b})$ as $\lambda \rightarrow \infty$ (Feydy et al., 2018). Thus, Energy Balancing Weights (Huling and Mak, 2020) are a special case of Causal Optimal Transport.

Optimal transport is also related to the mean maximum discrepancy (MMD) through the energy distance. The MMD is equal to

$$\mathcal{M} = 0.5 \int_{\mathcal{X} \times \mathcal{X}} k(x, x') d\phi(x),$$

for $\phi = \alpha - \beta$. For some reproducing kernel Hilbert space k and for a distance $d_{\mathcal{X}}$ defined as $d_{\mathcal{X}}(x, x') = \frac{1}{2} k(x, x') + \frac{1}{2} k(x, x') - k(x, x')$, MMD with kernel k is equivalent to the energy distance with distance $d_{\mathcal{X}}$ (Feydy et al., 2018) and, therefore, also to Causal Optimal Transport.

5 Simulation study

To evaluate the finite sample performance of the proposed weighting methodology, we use the simulation study originally presented in Hainmueller (2012). For each setting, we run 1000 experiments with a sample size of $n = 512$. The estimand of interest is the SATE.

5.1 Setup

Study design. We generate six covariates X_1, \dots, X_6 from the following distributions

$$\begin{aligned} \begin{bmatrix} X_1 \\ X_2 \\ X_3 \end{bmatrix} &\sim \mathcal{N} \left(\begin{bmatrix} 0 \\ 0 \\ 0 \end{bmatrix}, \begin{bmatrix} 2 & 1 & -1 \\ 1 & 1 & -0.5 \\ -1 & -0.5 & 1 \end{bmatrix} \right) \\ X_4 &\sim \text{Unif}(-3, 3) \\ X_5 &\sim \chi_1^2 \\ X_6 &\sim \text{Bern}(0.5). \end{aligned}$$

In this study, the last three covariates are mutually independent of each other and also of the first three covariates.

The treatment indicator is generated from

$$Z = \mathbb{I}(X_1 + 2X_2 - 2X_3 - X_4 - 0.5X_5 + X_6 + \nu > 0),$$

where ν is drawn from one of three distributions leading to different degrees of overlap:

High overlap	$\nu \sim \mathcal{N}(0, 100)$
Medium overlap	$\nu \sim g(\chi_5^2)$
Low overlap	$\nu \sim \mathcal{N}(0, 30)$.

The function g in the medium-overlap setting gives the χ_5^2 draws expectation 0.5 and variance 67.6. The distributions of the corresponding propensity scores for each setting are displayed in Figure 3, which is the same information as included in Figure 1 of Hainmueller (2012). We expect that the most difficult scenarios for estimating treatment effects to be in the low-overlap setting where there is a strong separation between treatment groups and in the medium-overlap setting where the errors are leptokurtic.

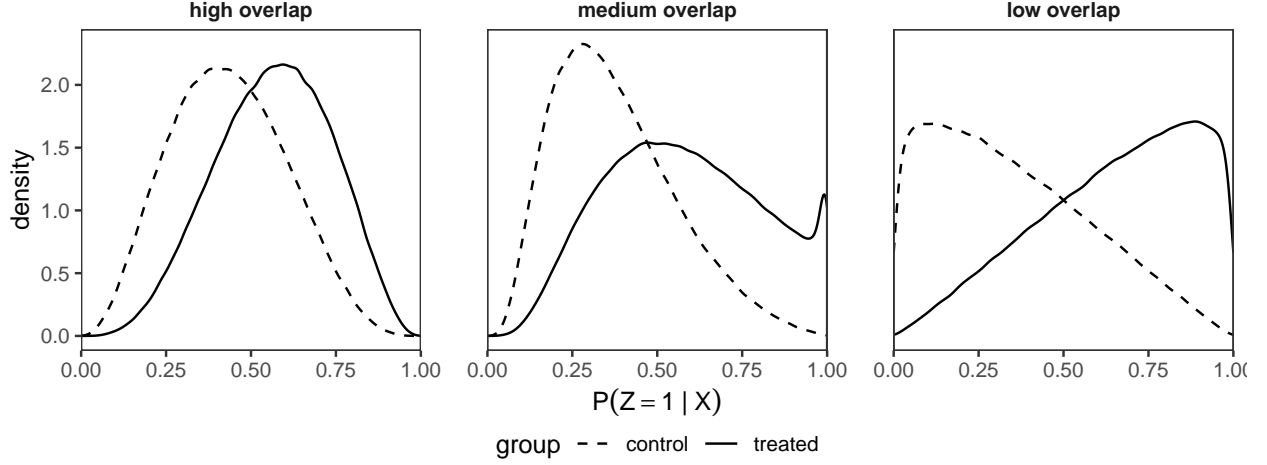


Figure 3: Propensity score distributions in the 3 overlap scenarios. The high overlap scenario corresponds to $\nu \sim \mathcal{N}(0, 100)$, the medium overlap scenario corresponds to $\nu \sim \chi_5^2$ scaled to have mean 0.5 and variance 67.6, and the low overlap scenario corresponds to $\nu \sim \mathcal{N}(0, 30)$.

Given the treatment indicator Z and the covariates X_1, \dots, X_6 , we simulate the outcome Y from one of two models:

$$(A) \ Y(0) = Y(1) = X_1 + X_2 + X_3 - X_4 + X_5 + X_6 + \eta$$

$$(B) \ Y(0) = Y(1) = (X_1 + X_2 + X_5)^2 + \eta,$$

with $\eta \sim \mathcal{N}(0, 1)$. There are two things to note about these outcome models. The first is that there is no effect of the treatment at the unit level and hence the SATE is 0. The second is that a linear outcome model should perform well in the first setting (A) while it should be biased in setting (B).

Methods under examination. We compare our methodology to several other weighting methods commonly used in the literature. The first method we consider is a logistic regression (GLM) using only first order terms. We also consider balancing methods such as the covariate balancing propensity score (CBPS), ran with the default settings provided by the corresponding R package (Fong et al., 2019), and the stable balancing weights (SBW) of Zubizarreta (2015) targeting mean balance. Finally, we also utilize SCM (Abadie and Gardeazabal, 2003).

For the Causal Optimal Transport (COT) weights, we utilize two variations. The first only balances the joint distribution (no constraints or “none”) and the second targets the joint distribution as well as mean balance (“means”). In both cases, we use an L_2 metric with standardized covariates. We use only the Sinkhorn Divergence version of Causal Optimal Transport from Eq. (10) since it has better convergence properties empirically. See Appendices A and C for more details.

5.2 Estimators

We consider three estimators to target the ATE estimand. The first is known as the Hájek estimator (Hajek, 1971) and is simply a weighted mean with sum to one weights as in Eq. (3). The second is an augmented or doubly robust estimator of Robins et al. (1994), and the third is a weighted least squares estimator—both only modeling linear terms of the covariates. We do not include a barycentric projection estimator since under an L_2 metric it gives the same result as the Hájek estimator.

5.3 Results

We now turn our attention to the results in the two outcome design settings: design A, where the linear outcome models are well-specified, and design B, where the linear outcome models are misspecified. Due to their nonparametric to semiparametric formulation, we expect Causal Optimal Transport to do better than other methods when the propensity score and outcome models are misspecified—the medium overlap scenario and in outcome model B.

Design A: well-specified outcome models. In this setting we expect that the estimation methods utilizing the true linear outcome model—*i.e.*, the augmented and weighted least squares estimators—will perform well for all weighting methods and that the Hájek weights will have worse performance as the overlap degrades.

We start by looking at the top half of Table 1. First, note that for Hájek estimators, Causal Optimal Transport and SBW have the lowest bias while, as expected, the augmented and weighted least squares estimators are roughly comparable across all weighting methods. In terms of root mean-squared error (RMSE), SBW performs the best in all overlap scenarios while Causal Optimal Transport with mean constraints performs the worst. Finally, note that the estimates are the same across all estimators for SBW, Causal Optimal Transport with constraints, and, amazingly, Causal Optimal Transport without constraints. This is because these methods exactly balance the outcome basis functions, which Causal Optimal Transport without balancing constraints does not even target explicitly. This is a feature of balancing distributions since it leads to the balance of functions of the covariates automatically. Similar results can be observed in Figure 4.

Design B: misspecified outcome models. Now, we turn to outcome setting B where the linear outcome models are misspecified and where none of the balancing functions include the correct basis functions. In this setting, we expect the outcome misspecification will increase bias but that Causal Optimal Transport will do better than the other methods in terms of bias and RMSE due to its nonparametric nature.

design	overlap	method	constraint	Bias			RMSE		
				Hajek	DR	WOLS	Hajek	DR	WOLS
A	high	GLM	none	0.01	0.00	0.00	0.13	0.10	0.10
		CBPS	means	0.16	0.00	0.00	0.21	0.10	0.10
		SBW	means	0.00	0.00	0.00	0.09	0.09	0.09
		SCM	none	0.09	0.00	0.00	0.17	0.14	0.14
		COT	none	0.00	0.00	0.00	0.10	0.10	0.10
			means	0.00	0.00	0.00	0.28	0.28	0.28
	medium	GLM	none	0.04	0.00	0.00	0.19	0.11	0.11
		CBPS	means	0.24	0.00	0.00	0.28	0.11	0.11
		SBW	means	0.00	0.00	0.00	0.10	0.10	0.10
		SCM	none	0.14	0.00	0.00	0.21	0.15	0.15
		COT	none	0.00	0.00	0.00	0.12	0.12	0.12
			means	0.02	0.02	0.02	0.28	0.28	0.28
	low	GLM	none	0.09	0.00	0.00	0.28	0.12	0.12
		CBPS	means	0.26	0.00	0.00	0.32	0.12	0.12
		SBW	means	0.00	0.00	0.00	0.11	0.11	0.11
		SCM	none	0.22	0.01	0.01	0.28	0.17	0.17
		COT	none	0.00	0.00	0.00	0.14	0.14	0.14
			means	-0.01	-0.01	-0.01	0.29	0.29	0.29
B	high	GLM	none	-0.01	-0.01	-0.02	1.18	1.14	1.14
		CBPS	means	0.24	-0.01	-0.02	1.12	1.11	1.09
		SBW	means	-0.01	-0.01	-0.01	1.00	1.00	1.00
		SCM	none	0.36	0.27	0.28	1.63	1.57	1.55
		COT	none	0.01	0.01	0.01	0.61	0.61	0.61
			means	0.01	0.01	0.01	0.42	0.42	0.42
	medium	GLM	none	1.12	1.10	1.04	1.72	1.69	1.70
		CBPS	means	1.20	1.06	0.95	1.72	1.64	1.56
		SBW	means	0.63	0.63	0.63	1.20	1.20	1.20
		SCM	none	1.19	1.12	1.10	2.05	1.97	1.95
		COT	none	0.23	0.23	0.23	0.74	0.74	0.74
			means	-0.03	-0.03	-0.03	0.43	0.43	0.43
	low	GLM	none	0.19	0.06	0.02	1.72	1.49	1.51
		CBPS	means	0.45	0.06	0.01	1.42	1.46	1.42
		SBW	means	0.03	0.03	0.03	1.03	1.03	1.03
		SCM	none	0.64	0.42	0.43	1.75	1.69	1.65
		COT	none	0.05	0.05	0.05	0.85	0.85	0.85
			means	0.00	0.00	0.00	0.41	0.41	0.41

Table 1: Performance of various weighting methods under the simulation settings of Hainmueller, 2012. Bold values are the values with the lowest bias or root mean-squared error (RMSE) of the methods under the same conditions. GLM refers to weighting by the inverse of the propensity score as calculated from a logistic regression model, CBPS is the covariate balancing propensity score, SBW is the stable balancing weights, SCM is the synthetic control method, and COT is the optimal transport formulation proposed in this paper. The estimators are Hajek weights (Hajek), doubly-robust augmented IPW (DR), and weighted least squares (WOLS). All weights are normalized to sum to 1. Constraints refer to balancing constraints and are one of "none" for no constraints or "mean" for mean constraints.

Indeed, the Causal Optimal Transport methods have the lowest RMSE across all overlap scenarios (see the lower half of Table 1 and Figure 5). Further, across the medium and low overlap settings, Causal Optimal Transport has the lowest bias as well; in the high overlap scenario, there is a negligible difference with Causal Optimal Transport, SBW, and GLM.

We again note that the Causal Optimal Transport gives estimates that do not vary between estimators. This is because the Causal Optimal Transport already balances the basis functions of the linear outcome model. Therefore, there is no difference between running an outcome regression utilizing linear terms of the covariates and the Hájek estimator.

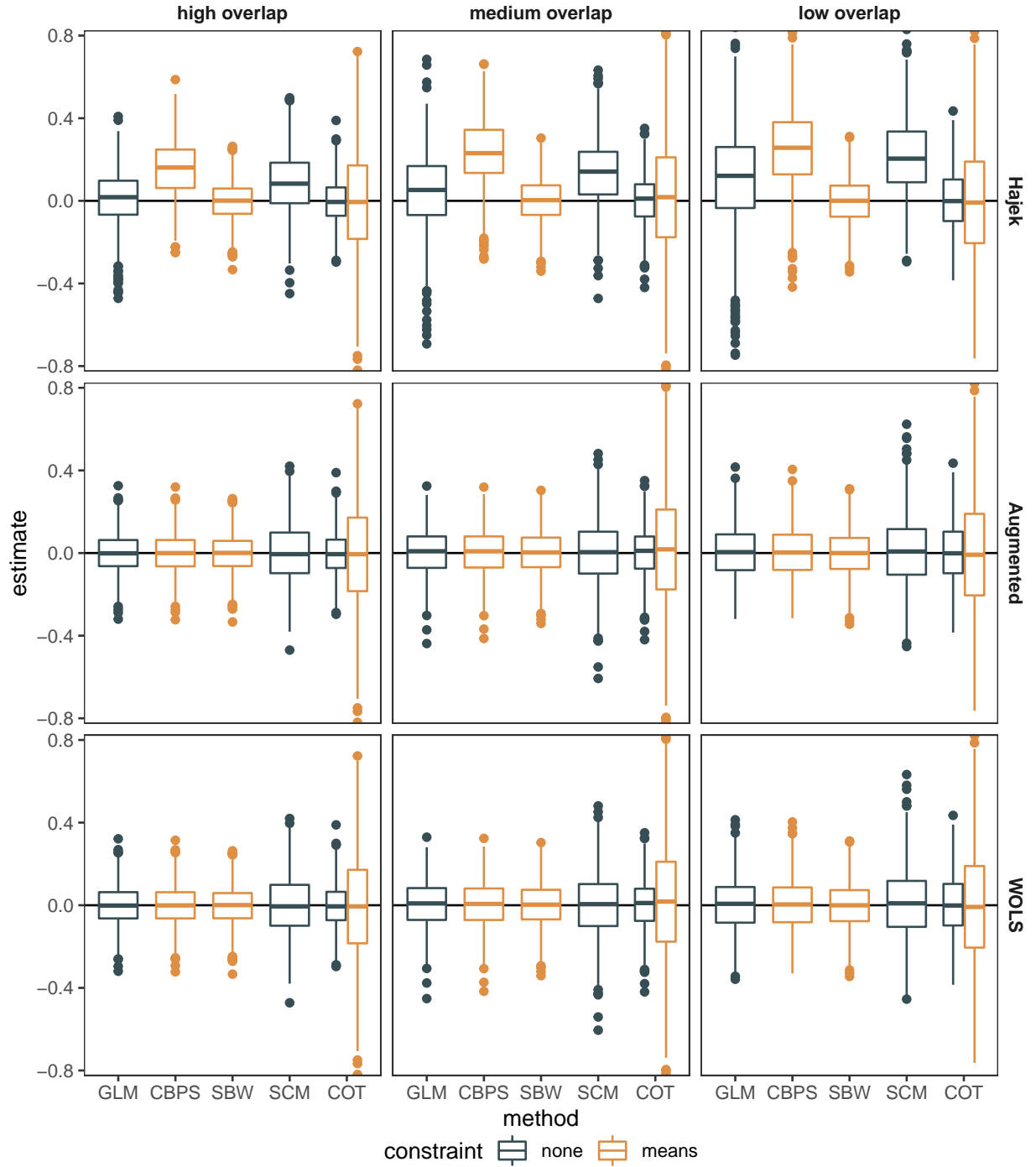


Figure 4: Boxplots of ATE estimation of various weighting methods under the simulation settings of Hainmueller (2012) for outcome design A, in which the outcomes are generated from a linear model. Constraints refer to constraints in the model and are one of “none” for no constraints and “means” for mean constraints. The black line denotes the true ATE. Note that the plots are zoomed in to better visualize the central parts of the distributions. Thus some outliers are not visible.

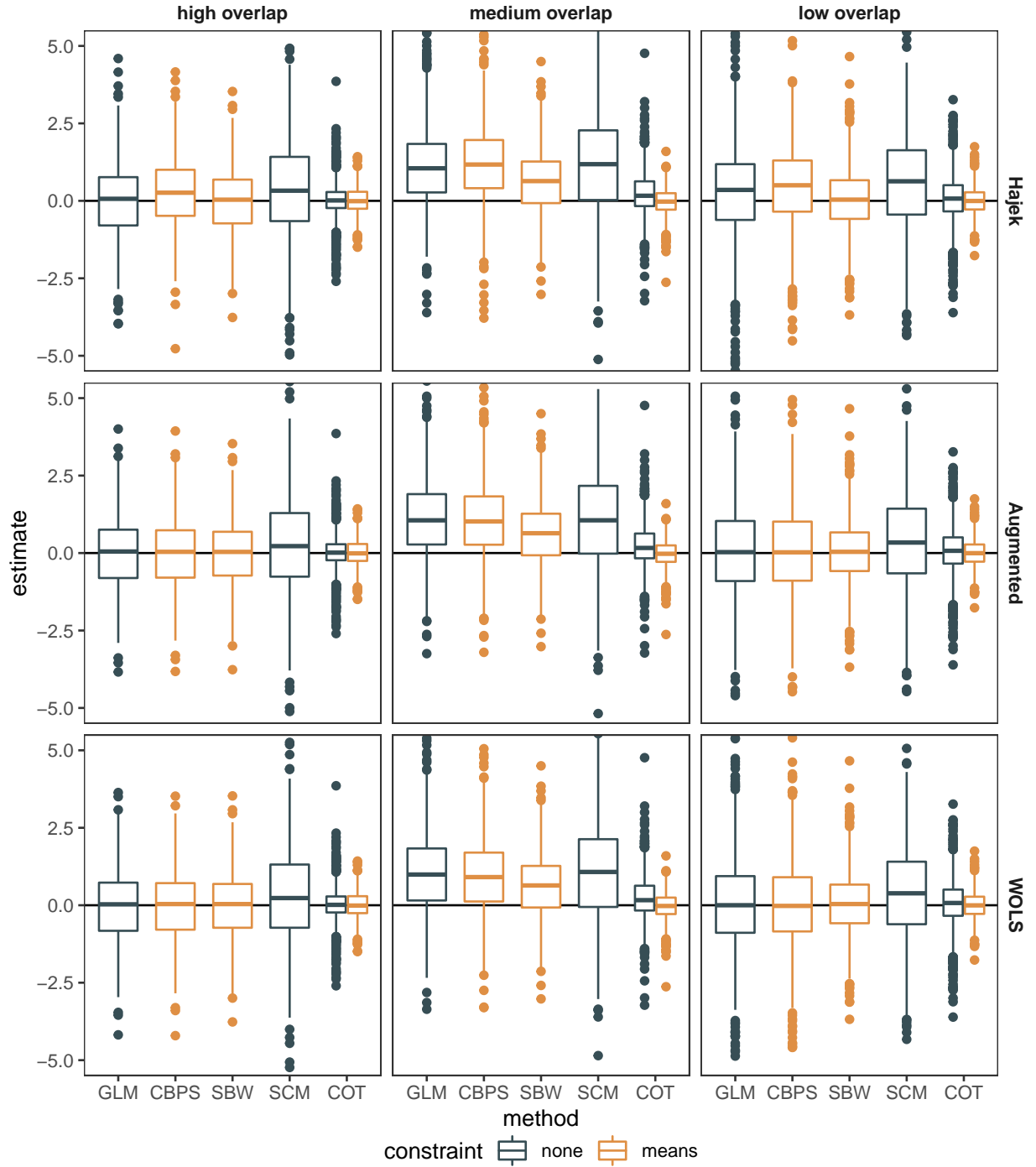


Figure 5: Boxplots of ATE estimation of various weighting methods under the simulation settings of Hainmueller (2012) for outcome design B, in which the outcomes are drawn from a non-linear outcome model. The dark line at 0 denotes the true treatment effect. Constraints refer to constraints in the model and are one of “none” for no constraints and “means” for mean constraints. Note that the plots have been zoomed in for better legibility and thus some outliers have been removed.

6 Case study

In this section, we turn to an application of our methodology to a real data set. There is growing interest in the literature to utilize libraries of RCTs to evaluate new interventions, the idea being that running new RCTs to evaluate every new intervention is expensive and time consuming. These studies, alternatively called an externally controlled trial or synthetic control group trial (U.S. Department of Health and Human Services Food and Drug Administration et al., 2001; Thorlund et al., 2020)—not to be confused with the synthetic control method of Abadie and Gardeazabal (2003)—compares a set of study subjects receiving a treatment to a group of individuals external to the trial at hand who did not receive the intervention of interest. The participants used for the control group can be taken from a variety of sources such as an observational study, electronic medical records, or from historical clinical trial data (Schmidli et al., 2020; Davi et al., 2020).

Our methodology allows researchers to adjust the distributions of the potential control groups from an external data source to form a suitable control group for the individuals receiving the intervention. To demonstrate this in practice, we present an analysis utilizing data from a multi-site RCT originally discussed by Blum et al. (2010).

For an additional data analysis using the LaLonde (1986) National Supported Work Demonstration program data, see Appendix D.

6.1 Misoprostol for the Treatment of Postpartum Hemorrhage

The original study was a double-blind, non-inferiority trial that exposed 31,055 women to prophylactic oxytocin during labor at five hospitals across Burkina Faso, Egypt, Turkey, and Vietnam. Women with uncontrolled blood-loss after delivery—a condition known as post-partum hemorrhage or PPH—were randomized to receive either 800 milligrams misoprostol (treatment condition) or 40 international units oxytocin (control condition). There were 407 and 402 women in each treatment group, respectively. The primary outcome for the study was whether blood loss was controlled within 20 minutes after PPH diagnosis. The authors discuss mean balance for several important confounders as a demonstration of the validity of the randomization. These confounders were the woman's age, whether the woman had no formal education, the number of live births, whether the woman was currently married, the fetus' gestational age, whether the woman had a previous PPH, hemoglobin in grams per liter, whether labor was induced, whether labor was augmented, whether the woman had an early cord clamp, whether there was controlled cord traction, whether the woman had a uterine massage, whether the placenta was delivered before the PPH diagnosis, and blood loss in milliliters (mL) at treatment.

6.2 Modifications and methods

We modify the study in a couple of ways to make it more similar to a external control trial using a library of RCTs. First, we modify the groups present in the study data. We do this by taking the largest site in the data, Egypt, and removing the control group. Then we take only the controls from the other four sites as if they were a potential comparison group from a library of RCTs to use for analyzing a new intervention. This step is justified since all of the sites were randomized independently and so there should be no interference between units across hospitals. One advantage of this approach is that we know the original treatment effect at the Egypt site, so we can evaluate how well our method performs relative to the ground truth. If Causal Optimal Transport can recover the original treatment effect, we know it is performing well.

Second, instead of whether blood loss was controlled after 20 minutes, we use the difference in observed blood loss between treatment groups measured after 20 minutes as our causal estimand of interest. The original treatment effect observed at the Egypt site was a difference of 0.369 mL in blood loss between treatment groups with a confidence interval of $(-27.1 \text{ mL}, 27.8 \text{ mL})$.

To estimate treatment effects, we use Causal Optimal Transport with hyperparameter tuning as in Algorithm 1 and an L_2 norm on covariates. Our estimators are a Hájek estimator, an augmented estimator using a Gaussian process with a squared-exponential covariance kernel, weighted least squares, and a barycentric projection estimator as in Eq. (8) but using an L_1 metric.

For our estimates to be valid, we require that there be no unmeasured confounding but also that the estimates are “transportable,” *i.e.* we are able to take estimates from the other hospitals in the external control group and “transport” them to Egypt. This requires that conditional on the observed covariates there are no other variables that can effect the outcome and treatment indicator (d -separation holds, Pearl and Bareinboim, 2013).

6.3 Design diagnostics

Prior to discussing outcome results, we discuss the level of balance achieved by our methodology. Typically, researchers examine mean balance diagnostics to assess the performance of a weighting or matching estimator (Stuart, 2010). We present the results of such diagnostics in Figure 6 for the Causal Optimal Transport weights. In the figure, we can see that mean balance is improved but that substantial biases still remain. As such, we might expect that methods balancing the means of the covariates will perform poorly.

Similarly, we present results for the change in 2-Sinkhorn divergence across the two methods before and after weighting. In every case, distributional balance is improved (Figure 7). The distributional balance is slightly better without mean constraints, indicating we pay a slight penalty for the additional constraints.

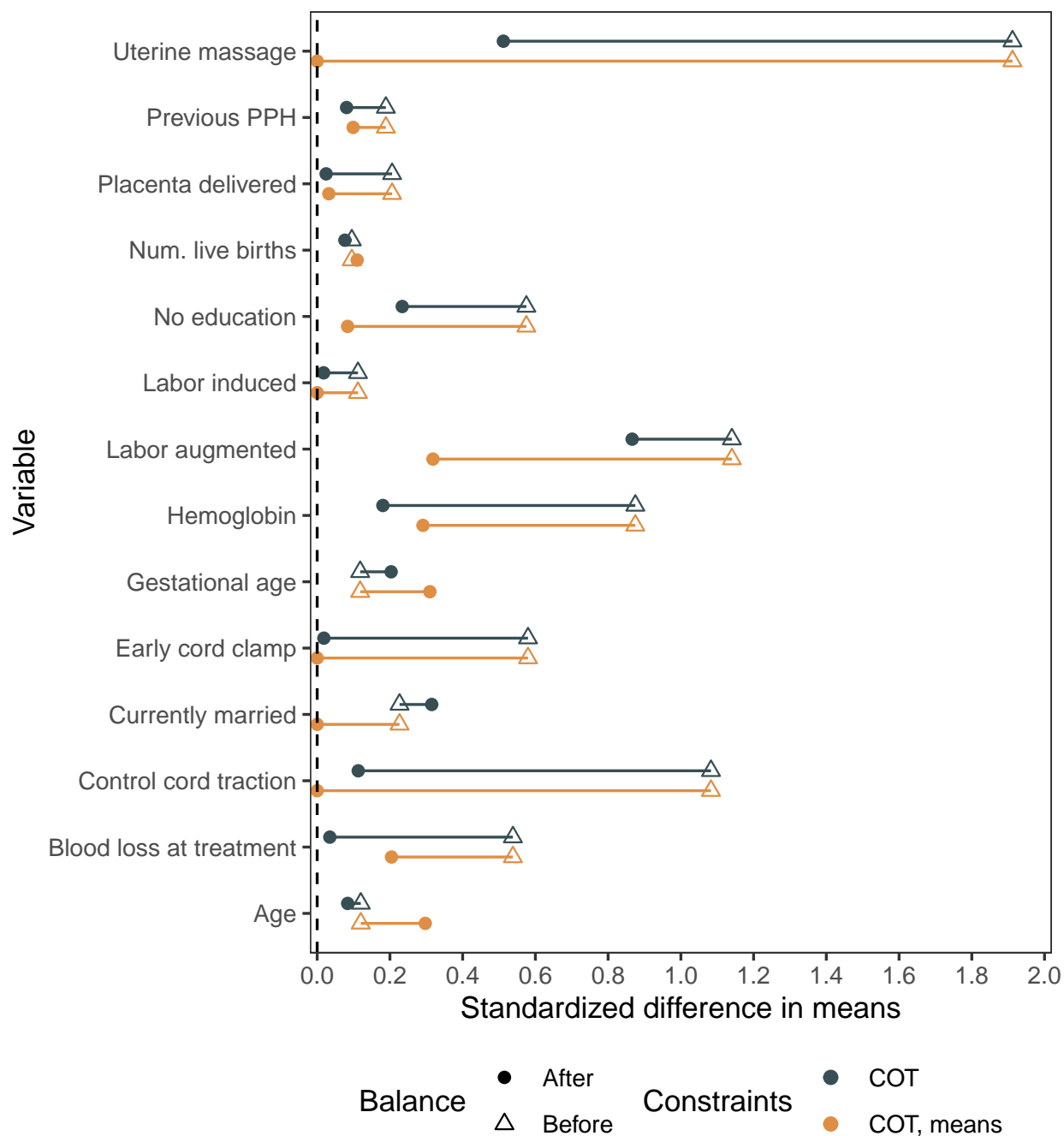


Figure 6: Change in the standardized difference in means between the two groups before and after weighting. An examination in the change in balance before and after utilizing the optimal transport methods with the listed constraints for the misoprostol receiving participants in Egypt versus the oxytocin receiving participants at the other sites. “COT” corresponds to no constraints and “COT, means” corresponds to constraints on mean balance.

6.4 Case study results

Amazingly, one of the Causal Optimal Transport methods recovered the original treatment estimate, demonstrating the utility of this methodology for externally controlled trials. For Causal Optimal Transport with no

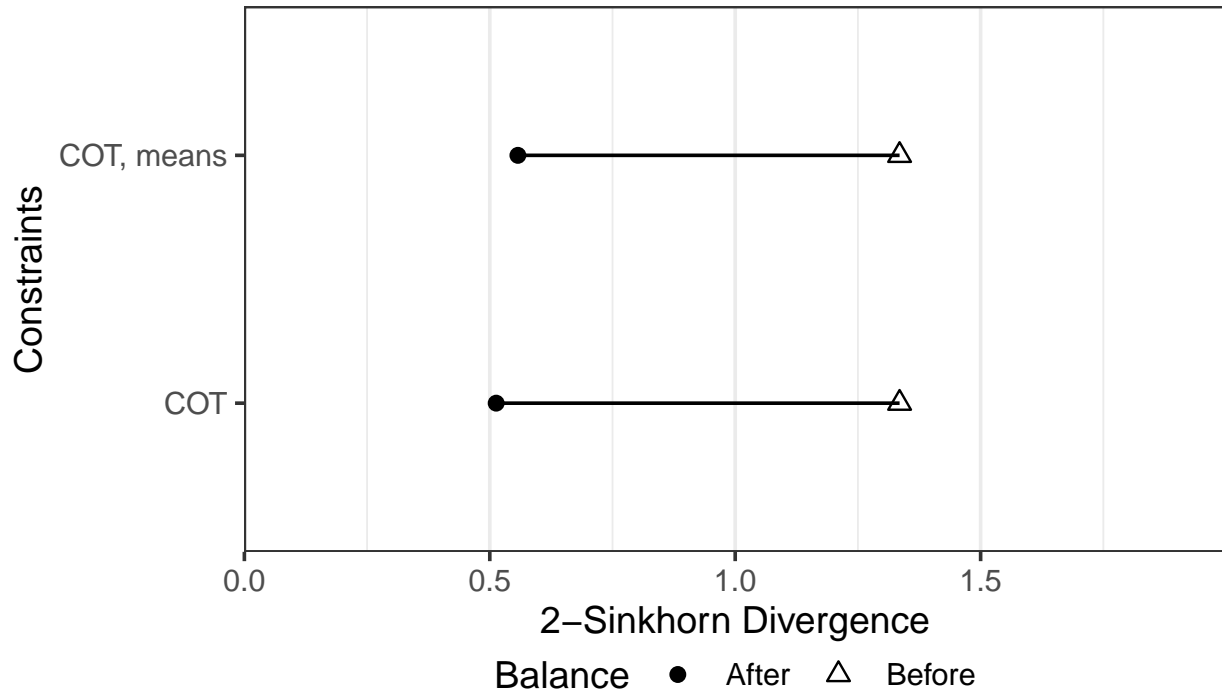


Figure 7: Change in the 2-Sinkhorn divergence between the two groups before and after weighting. An examination in the change in balance before and after utilizing the optimal transport methods with the listed constraints for the misoprostol receiving participants in Egypt versus the oxytocin receiving participants at the other sites. "COT" corresponds to no constraints and "COT, means" corresponds to constraints on the mean balance.

constraints, all estimators have negative biases but the confidence intervals cover the observed estimate in the original RCT in every case.

Unfortunately, the mean balancing formulations of Causal Optimal Transport display substantial biases in their estimates and none of the confidence intervals cover the original estimate, as we expected (Row 2 of Table 2). Figure 8 also displays these results graphically.

Method	Hajek		Augmented		Weighted OLS		Barycentric projection	
	Est.	C.I.	Est.	C.I.	Est.	C.I.	Est.	C.I.
COT	-11.0	(-30.3, 8.3)	-19.4	(-38.8, 0.0)	-40.6	(-145.9, 64.7)	-9.5	(-30.5, 11.5)
COT, means	-108.9	(-128.1, -89.8)	-99.4	(-119.6, -79.2)	-103.6	(-175.3, -31.8)	-108.8	(-129.8, -87.8)

Table 2: Estimates and confidence intervals for optimal transport weighting methods applied to a modification of the data in Blum et al., 2010. We have constructed a control group for the misoprostol receiving patients at Egyptian site using the controls from the four other sites. The original treatment effect at the Egypt site was 0.369 mL with a 95% C.I. of $(-27.1, 27.8)$. The augmented method uses a gaussian process as the outcome model.

7 Summary and remarks

We have provided a new tool for the estimation of causal effects in observational studies: Causal Optimal Transport. This method allows for checks of distributional overlap and model-free weight estimation that

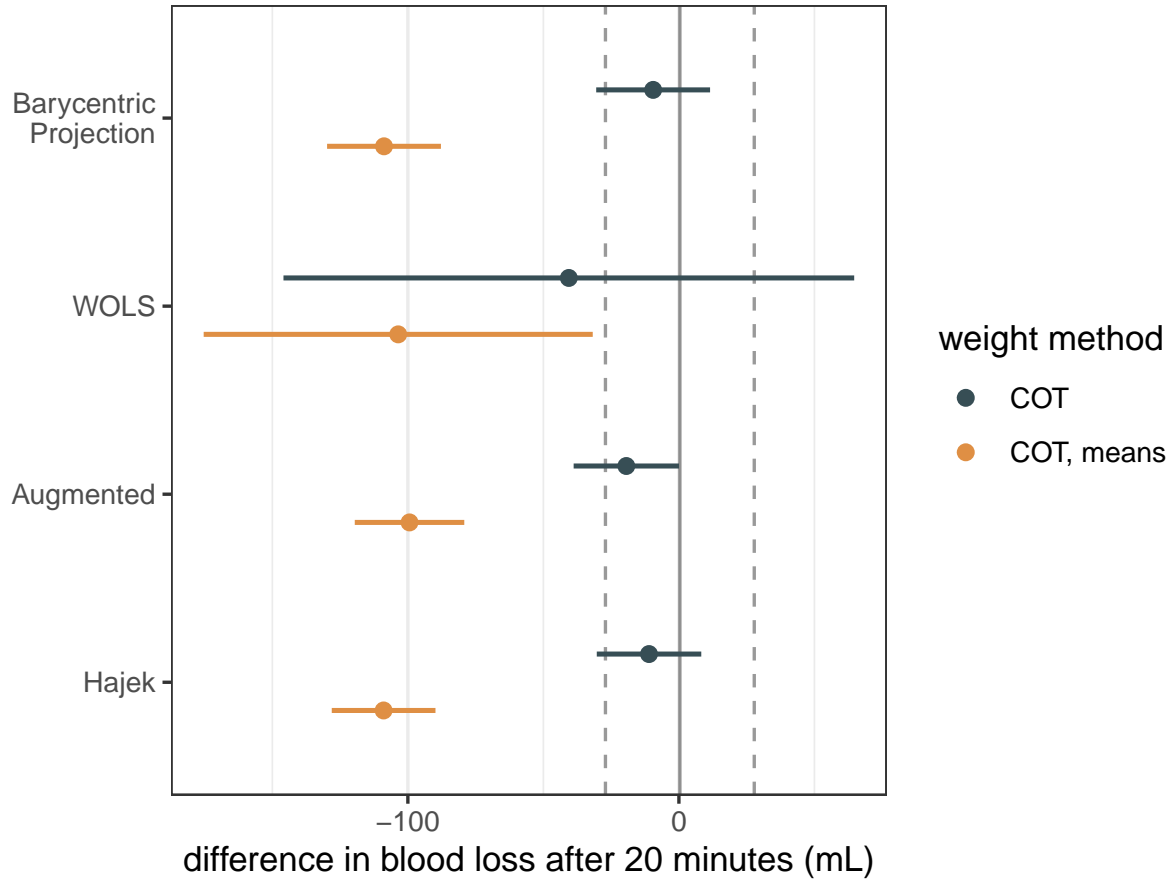


Figure 8: Results for treatment effect estimation between the treated misoprostol group in Egypt versus the control oxytocin group at four other sites. We see that methods without mean constraints are able to recover the effect estimate. Note that “COT” corresponds to no constraints and “COT, means” corresponds to constraints on mean balance.

is semiparametrically efficient. We also showed how several other methods for causal inference are closely related to Causal Optimal Transport and that Causal Optimal Transport can be seen as a generalization of these methods. In our simulation study, we also demonstrated that this methodology is beneficial when both the outcome models and propensity score models are misspecified. Compared to other common weighting methods, Causal Optimal Transport generally has lower bias and lower root mean-squared error.

There are several areas for future research. For one, we would like to explore the sensitivity of the method to the choice of cost function. Second, selecting covariates through typical model selection frameworks such as an L_1 penalized regression is not obvious given that Causal Optimal Transport does not generate clear predictive models. Third, more work needs to be done to extend this framework to time series data.

Acknowledgements

The author would like to thank Claire Chaumont, Gang Liu, Aarón Sonabend, Lorenzo Trippa, and José Zubarreta for helpful comments and feedback on an earlier version of this manuscript.

Funding

This research was funded by NIH grant 5T32CA009337-40 and the David Geffen Scholarship.

References

- Abadie, Alberto and Javier Gardeazabal (2003). "The Economic Costs of Conflict : A Case Study of the Basque Country". In: *The American Economic Review* 93.1, pp. 113–132 (see pp. [13](#), [17](#), [22](#)).
- Altschuler, Jason, Jonathan Weed, and Philippe Rigollet (2017). "Near-linear time approximation algorithms for optimal transport via Sinkhorn iteration". In: *Advances in Neural Information Processing Systems* 2017-Decem.1, pp. 1965–1975 (see pp. [7](#), [12](#)).
- Ambrosio, Luigi, Nicola Gigli, and Giuseppe Savare (2005). *Gradient Flows in Metric Spaces and in the Space of Probability Measures*. Series Title: Lectures in Mathematics ETH Zürich. Basel: Birkhäuser-Verlag. DOI: [10.1007/b137080](#). URL: <http://link.springer.com/10.1007/b137080> (see p. [8](#)).
- Armijo, Larry (Jan. 1, 1966). "Minimization of functions having Lipschitz continuous first partial derivatives". In: *Pacific Journal of Mathematics* 16.1, pp. 1–3. DOI: [10.2140/pjm.1966.16.1](#). URL: <http://msp.org/pjm/1966/16-1/p01.xhtml> (visited on 12/02/2021).
- Blondel, Mathieu, Vivien Seguy, and Antoine Rolet (2018). "Smooth and sparse optimal transport". In: *International Conference on Artificial Intelligence and Statistics, AISTATS 2018* 84, pp. 880–889 (see pp. [7](#), [12](#), [33](#), [34](#), [39](#)).
- Blum, Jennifer et al. (2010). "Treatment of post-partum haemorrhage with sublingual misoprostol versus oxytocin in women receiving prophylactic oxytocin : a double-blind , randomised , non-inferiority trial". In: *The Lancet* 375.9710. Publisher: Elsevier Ltd, pp. 217–223. DOI: [10.1016/S0140-6736\(09\)61923-1](#). URL: [http://dx.doi.org/10.1016/S0140-6736\(09\)61923-1](http://dx.doi.org/10.1016/S0140-6736(09)61923-1) (see pp. [22](#), [25](#)).
- Cuturi, Marco (June 4, 2013). "Sinkhorn Distances: Lightspeed Computation of Optimal Transport". In: *Advances in Neural Information Processing Systems*. Ed. by C J C Burges et al. Vol. 26. Curran Associates, Inc., pp. 1–9 (see pp. [7](#), [12](#)).
- Davi, Ruthie et al. (2020). "Informing single-arm clinical trials with external controls". In: *Nature reviews. Drug discovery* 19.12. Publisher: Springer US, pp. 821–822. DOI: [10.1038/d41573-020-00146-5](#). URL: <http://dx.doi.org/10.1038/d41573-020-00146-5> (see p. [22](#)).
- Dvurechensky, Pavel, Alexander Gasnikov, and Alexey Kroshnin (2018). "Computational Optimal Transport: Complexity by Accelerated Gradient Descent Is Better Than by Sinkhorn's Algorithm". In: *35th International Conference on Machine Learning, ICML 2018* 3. ISBN: 9781510867963, pp. 2196–2220 (see p. [12](#)).
- Fan, Jianqing et al. (2016). "Improving Covariate Balancing Propensity Score : A Doubly Robust and Efficient Approach". In: *Mimeo*, pp. 1–47 (see p. [2](#)).
- Feydy, Jean et al. (2018). "Interpolating between optimal transport and mmd using sinkhorn divergences". In: *arXiv* 89 (see pp. [8](#), [12](#), [15](#), [35](#), [41](#)).

- Fidler, Matthew L. et al. (2020). *lbfgsb3c: Limited Memory BFGS Minimizer with Bounds on Parameters withoptim() 'C' Interface*. URL: <https://CRAN.R-project.org/package=lbfgsb3c> (see p. 12).
- Fong, Christian, Marc Ratkovic, and Kosuke Imai (2019). *CBPS: Covariate Balancing Propensity Score*. URL: <https://cran.r-project.org/package=CBPS> (see p. 17).
- Fournier, Nicolas and Arnaud Guillin (2015). "On the rate of convergence in Wasserstein distance of the empirical measure". In: *Probability Theory and Related Fields* 162.3, pp. 707–738. DOI: [10.1007/s00440-014-0583-7](https://doi.org/10.1007/s00440-014-0583-7) (see pp. 7, 37, 40).
- Frank, Marguerite and Philip Wolfe (Mar. 1956). "An algorithm for quadratic programming". In: *Naval Research Logistics Quarterly* 3.1, pp. 95–110. DOI: [10.1002/nav.3800030109](https://doi.org/10.1002/nav.3800030109). URL: <http://doi.wiley.com/10.1002/nav.3800030109> (see p. 12).
- Genevay, Aude, Gabriel Peyré, and Marco Cuturi (2018a). "Learning Generative Models with Sinkhorn Divergences". In: *AISTATS*, p. 10 (see p. 7).
- Genevay, Aude et al. (2018b). "Sample complexity of sinkhorn divergences". In: *arXiv*. URL: <http://arxiv.org/abs/1810.02733> (see pp. 7, 41, 42).
- Hahn, Jinyong (1998). "On the Role of the Propensity Score in Efficient Semiparametric Estimation of Average Treatment Effects". In: *Econometrica* 66.2, pp. 315–331 (see p. 11).
- Hainmueller, Jens (2012). "Entropy balancing for causal effects: A multivariate reweighting method to produce balanced samples in observational studies". In: *Political Analysis* 20.1, pp. 25–46. DOI: [10.1093/pan/mpr025](https://doi.org/10.1093/pan/mpr025) (see pp. 2, 16, 19–21).
- Hajek, J. (1971). "Comment on "Comment on An essay on the logical foundations of survey sampling"". In: *Foundations of Statistical Inference*. Ed. by V.P. Godambe and D.A. Sprott. Holt, Rinehart and Winston, pp. 201–233 (see p. 18).
- Huling, Jared D and Simon Mak (2020). "Energy Balancing of Covariate Distributions". In: (see pp. 12, 15, 35).
- Imai, Losuke and Marc Ratkovic (2014). "CBPS: Covariate Balancing Propensity Score". In: pp. 243–263. URL: <https://cran.r-project.org/package=CBPS> (see pp. 2, 3).
- Kallus, Nathan (2016). "Generalized Optimal Matching Methods for Causal Inference". In: URL: <http://arxiv.org/abs/1612.08321> (see p. 2).
- Kallus, Nathan, Brenton Pennicooke, and Michele Santacatterina (2018). "More robust estimation of sample average treatment effects using Kernel Optimal Matching in an observational study of spine surgical interventions". In: (April), pp. 1–37 (see p. 2).
- Kallus, Nathan and Michele Santacatterina (2019). "Kernel Optimal Orthogonality Weighting: A Balancing Approach to Estimating Effects of Continuous Treatments". In: URL: <http://arxiv.org/abs/1910.11972> (see p. 2).

- Kang, Joseph D.Y. and Joseph L. Schafer (2007). "Demystifying double robustness: A comparison of alternative strategies for estimating a population mean from incomplete data". In: *Statistical Science* 22.4, pp. 523–539. DOI: [10.1214/07-STS227](https://doi.org/10.1214/07-STS227) (see p. 2).
- Kantorovich, L. (1942). "On the transfer of masses (in Russian)". In: *Doklady Akademii Nauk* 37.2, pp. 227–229 (see p. 7).
- LaLonde, Robert J. (1986). "American Economic Association Evaluating the Econometric Evaluations of Training Programs with Experimental Data Author (s): Robert J . LaLonde Source : The American Economic Review , Vol . 76 , No . 4 (Sep . , 1986) , pp . 604-620 Published by : Americ". In: *The American Economic Review* 76.4, pp. 604–620 (see pp. 22, 45).
- Li, Yan and Liang Li (Feb. 1, 2021). "Propensity score analysis methods with balancing constraints: A Monte Carlo study". In: *Statistical Methods in Medical Research*. DOI: [10.1177/0962280220983512](https://doi.org/10.1177/0962280220983512). URL: <http://journals.sagepub.com/doi/10.1177/0962280220983512> (see p. 2).
- Mena, Gonzalo and Jonathan Weed (2019). "Statistical bounds for entropic optimal transport: sample complexity and the central limit theorem". In: pp. 1–23. URL: <http://arxiv.org/abs/1905.11882> (see pp. 7, 41, 42).
- Monge, Gaspard (1781). *Mémoire sur la théorie des déblais et des remblais*. De l'Imprimerie Royale (see p. 6).
- MOSEK ApS (2021). *The MOSEK optimization toolbox for R manual. Version 9.2*. URL: <https://docs.mosek.com/9.2/rmosek/index.html> (see p. 12).
- Owen, Art B. (2013). "9: Importance Sampling". In: *Monte Carlo theory, methods and examples* (see p. 33).
- Paszke, Adam et al. (2019). "PyTorch: An Imperative Style, High-Performance Deep Learning Library". In: *Advances in Neural Information Processing Systems* 32. Ed. by H. Wallach et al. Curran Associates, Inc., pp. 8024–8035. URL: <http://papers.neurips.cc/paper/9015-pytorch-an-imperative-style-high-performance-deep-learning-library.pdf> (see p. 12).
- Pearl, Judea and Elias Bareinboim (2013). "Transportability across studies: A formal approach introduction". In: *Technical Report No. R372* (April), pp. 1–18 (see p. 23).
- Perrot, Michael et al. (2016). "Mapping estimation for discrete optimal transport". In: *Advances in Neural Information Processing Systems* (Nips), pp. 4204–4212 (see p. 13).
- Peyré, Gabriel and Marco Cuturi (2019). "Computational Optimal Transport". In: *Foundations and Trends in Machine Learning* 11.5. ISBN: 2200000073, pp. 355–607. DOI: [10.1561/2200000073](https://doi.org/10.1561/2200000073) (see pp. 6, 7).
- Ratkovic, Marc and Dustin Tingley (Mar. 16, 2017). "Estimation and Inference on Nonlinear and Heterogeneous Effects". In: URL: <http://arxiv.org/abs/1703.05849> (see p. 2).

- Robins, James M., Andrea Rotnitzky, and Lue Ping Zhao (1994). "Estimation of regression coefficients when some regressors are not always observed". In: *Journal of the American Statistical Association* 89.427, pp. 846–866. DOI: [10.1080/01621459.1994.10476818](https://doi.org/10.1080/01621459.1994.10476818) (see pp. [1](#), [18](#)).
- Rosenbaum, Paul R (1987). "Model-Based Direct Adjustment". In: 82.398, pp. 387–394 (see p. [1](#)).
- (1989). "Optimal matching for observational studies". In: *Journal of the American Statistical Association* 84.408, pp. 1024–1032. DOI: [10.1080/01621459.1989.10478868](https://doi.org/10.1080/01621459.1989.10478868) (see pp. [7](#), [13](#)).
- Rosenbaum, Paul R. and Donald B. Rubin (1983). "The Central Role of the Propensity Score in Observational Studies for Causal Effects". In: *Biometrika* 70.1, pp. 41–55 (see pp. [1](#), [5](#)).
- Rotnitzky, Andrea, James M. Robins, and Daniel O. Scharfstein (1998). "Semiparametric Regression for Repeated Outcomes with Nonignorable Nonresponse". In: *Journal of the American Statistical Association* 93.444, pp. 1321–1339. DOI: [10.1080/01621459.1998.10473795](https://doi.org/10.1080/01621459.1998.10473795) (see p. [1](#)).
- Rubin, Donald B (1986). "Cormment: Which Ifs Have Causal Answers". In: 81.396, pp. 961–962 (see p. [5](#)).
- (1974). "Estimating causal effects of treatments in randomized and nonrandomized studies." In: *Journal of Educational Psychology* 66.5, pp. 668–701. (Visited on 04/12/2014) (see p. [4](#)).
- Schmidli, Heinz et al. (2020). "Beyond Randomized Clinical Trials: Use of External Controls". In: *Clinical Pharmacology and Therapeutics* 107.4, pp. 806–816. DOI: [10.1002/cpt.1723](https://doi.org/10.1002/cpt.1723) (see p. [22](#)).
- Solomon, J et al. (2015). "Convolutional Wasserstein Distances: Efficient Optimal Transportation on Geometric Domains". In: *Acm Transactions on Graphics* 34.4. ISBN: 0730-0301, p. 11. DOI: [10.1145/2766963](https://doi.org/10.1145/2766963) (see p. [7](#)).
- Splawa-Neyman, Jerzy (1923). "On the Application of Probability Theory to Agricultural Experiments. Essay on Principles. Section 9". In: *Roczniki Nauk Rolniczych Tom X*, pp. 1–51. DOI: [10.1214/ss/1177012031](https://doi.org/10.1214/ss/1177012031). URL: <https://projecteuclid.org/journals/statistical-science/volume-5/issue-4/On-the-Application-of-Probability-Theory-to-Agricultural-Experiments-Essay/10.1214/ss/1177012031.full> (see p. [4](#)).
- Stuart, Elizabeth A. (2010). "Matching Methods for Causal Inference: A Review and a Look Forward". In: *Statistical Science* 25.1. ISBN: 0883-4237 (Print)\r0883-4237 (Linking), pp. 1–21. DOI: [10.1214/09-STS313](https://doi.org/10.1214/09-STS313). URL: <http://projecteuclid.org/euclid.ss/1280841730> (see p. [23](#)).
- Thorlund, Kristian et al. (2020). "Synthetic and external controls in clinical trials – A primer for researchers". In: *Clinical Epidemiology* 12, pp. 457–467. DOI: [10.2147/CLEP.S242097](https://doi.org/10.2147/CLEP.S242097) (see p. [22](#)).
- U.S. Department of Health and Human Services Food and Drug Administration, Center for Drug Evaluation and Research (CDER), and Center for Biologics Evaluation and Research (CBER) (2001). *Guidance for Industry: E 10 Choice of Control Group and Related Issues in Clinical Trials*. Issue: May, pp. 1–33 (see p. [22](#)).

- Ushey, Kevin, J. J. Allaire, and Yuan Tang (2021). *reticulate: Interface to 'Python'*. URL: <https://CRAN.R-project.org/package=reticulate>.
- Villani, Cedric (2006). *Optimal transport, old and new*. Springer (see pp. 34, 35).
- Wang, Yixin and Jose R Zubizarreta (2019a). “Minimal dispersion approximately balancing weights: asymptotic properties and practical considerations”. In: *Biometrika*. DOI: [10.1093/biomet/asz050](https://doi.org/10.1093/biomet/asz050) (see p. 2).
- Wang, Yixin and José R. Zubizarreta (2019b). “Large Sample Properties of Matching for Balance”. In: pp. 1–25. URL: <http://arxiv.org/abs/1905.11386> (see p. 9).
- Weed, Jonathan and Francis Bach (2017). “Sharp asymptotic and finite-sample rates of convergence of empirical measures in Wasserstein distance”. In: pp. 1–35. URL: <http://arxiv.org/abs/1707.00087> (see p. 7).
- Wong, Raymond K.W. and Kwun Chuen Gary Chan (2018). “Kernel-based covariate functional balancing for observational studies”. In: *Biometrika* 105.1, pp. 199–213. DOI: [10.1093/biomet/asx069](https://doi.org/10.1093/biomet/asx069) (see p. 2).
- Zubizarreta, José R. (2012). “Using mixed integer programming for matching in an observational study of kidney failure after surgery”. In: *Journal of the American Statistical Association* 107.500, pp. 1360–1371. DOI: [10.1080/01621459.2012.703874](https://doi.org/10.1080/01621459.2012.703874) (see pp. 2, 15).
- (2015). “Stable Weights that Balance Covariates for Estimation With Incomplete Outcome Data”. In: *Journal of the American Statistical Association* 110.511, pp. 910–922. DOI: [10.1080/01621459.2015.1023805](https://doi.org/10.1080/01621459.2015.1023805) (see pp. 3, 17).

A Convergence

In this section, we prove the convergence of our estimator and provide a simulation study that demonstrates this convergence. First, we need the following lemma.

Lemma 1 (The importance sampling weights converge to β)

Let Assumptions 2 and 3 hold. Define the importance sampling weights as $\check{w}_i^* = \frac{d\beta(X_i)}{d\alpha(X_i)}$ and define the self-normalized importance sampling weights as

$$w_i^* = \frac{\frac{1}{n} \check{w}_i^*}{\sum_i \frac{1}{n} \check{w}_i^*}.$$

Then,

$$\mathbf{w}^* \rightharpoonup \beta.$$

Proof. By Assumptions 2 and 3, \check{w}_i^* exists for all i . Then define $\mathbb{P}_n(X \in E) = \sum_i \mathbb{I}(X_i \in E) w_i^*$, for some $E \subset \mathcal{X}$. Take $f(X) = \mathbb{I}(X \in E)$. By Theorem 9.2 in Owen (2013), $\mathbb{P}_n(X \in E) = \sum_i f(X_i) w_i^* \xrightarrow{\text{a.s.}} \mathbb{E}_\beta(f(X)) = \int_{\mathcal{X}} f d\beta = \mathbb{P}_\beta(X \in E)$, where $\mathbb{P}_\beta(\cdot)$ denotes the probability of $X \in E$ when $X \sim \beta$. Thus we have $\lim_{n \rightarrow \infty} \mathbb{P}_n(X \in E) = \mathbb{P}_\beta(X \in E)$. \square

A.1 Proof of Theorem 1

We now offer our proof of Theorem 1. We first define some additional notation to make the work a little simpler. As a reminder, $\text{OT}_\lambda(\mathbf{a}, \mathbf{b})$ denotes the objective in Eq. (7) and $S_\lambda(\mathbf{a}, \mathbf{b})$ is the Sinkhorn Divergence. The basic idea is that the objective using Causal Optimal Transport weights will always be less than the objective function using the importance sampling weights \mathbf{w}^* . In turn, this latter quantity goes to 0, implying that the Causal Optimal Transport weights converge to β .

Proof. We begin by proving the L_2 regularized weights converge, then the entropically regularized weights, and finally, the Sinkhorn divergence. We also have that under Assumptions 2 and 3, \mathbf{w}^* exists. Then by Lemma 1, $\mathbf{w}^* \rightharpoonup \beta$.

L_2 penalization. Theorem 1 of Blondel et al. (2018) give bounds on $\text{OT}_\lambda(\mathbf{a}, \mathbf{b})$:

$$\frac{\lambda}{2} \sum_{i,j} \left(\frac{\mathbf{a}_i}{n} + \frac{\mathbf{b}_j}{m} - \frac{1}{mn} \right)^2 \leq \text{OT}_\lambda(\mathbf{w}^*, \mathbf{b}) - \text{OT}(\mathbf{a}, \mathbf{b}) \leq \frac{\lambda}{2} \min\{\|\mathbf{a}\|^2, \|\mathbf{b}\|^2\}. \quad (13)$$

Then the upper bounds on the L_2 regularized problem for the importance sampling weights are

$$\text{OT}_\lambda(\mathbf{a}, \mathbf{b}) \leq \text{OT}(\mathbf{w}^*, \mathbf{b}) + \frac{\lambda}{2} \|\mathbf{b}\|,$$

where the first inequality follows from rearrangement of Eq. (13) and the fact that $\min\{\|\mathbf{w}^*\|^2, \|\mathbf{b}\|^2\}$ is minimized by the measure where all the observations have the same weight. Also,

$$\|\mathbf{b}\|^2 = \sum_j \mathbf{b}_j^2 = \frac{1}{m} \rightarrow 0.$$

Thus, $\text{OT}_\lambda(\mathbf{w}^*, \mathbf{b}) \rightarrow \text{OT}(\mathbf{w}^*, \mathbf{b})$ and by Corollary 6.9 of Villani (2006), $\text{OT}(\mathbf{w}^*, \mathbf{b}) \rightarrow 0$.

Now we turn directly to the Causal Optimal Transport weights. The problem is convex (Blondel et al., 2018), which means that

$$\text{OT}_\lambda(\mathbf{w}_{\text{COT}}, \mathbf{b}) \leq \text{OT}_\lambda(\mathbf{c}, \mathbf{b})$$

for all $\mathbf{c} \in \Delta_n$ that satisfy the constraints of the problem. Further, Assumption 4.3 means that $\exists n > 0$ such that the importance sampling weights \mathbf{w}^* also satisfy the balancing constraints. This means that

$$\text{OT}_\lambda(\mathbf{w}_{\text{COT}}, \mathbf{b}) \leq \text{OT}_\lambda(\mathbf{w}^*, \mathbf{b})$$

and both quantities also satisfy the problem constraints for some n .

Finally, if $\text{OT}_\lambda(\mathbf{w}_{\text{COT}}, \mathbf{b})$ goes to 0, this will mean $\mathbf{w}_{\text{COT}} \rightarrow \beta$ since $\text{OT}_\lambda(\mathbf{w}_{\text{COT}}, \mathbf{b}) \rightarrow \text{OT}(\mathbf{w}_{\text{COT}}, \mathbf{b})$. Thus, since $\text{OT}_\lambda(\mathbf{w}_{\text{COT}}, \mathbf{b}) \rightarrow 0$ because $\text{OT}_\lambda(\mathbf{w}^*, \mathbf{b})$ goes to 0, by Corollary 6.9 in Villani (2006)

$$\mathbf{w}_{\text{COT}} \rightarrow \beta.$$

Entropy penalization. The entropy penalized Causal Optimal Transport problem is also a convex problem, which allows us to conclude

$$\text{OT}_\lambda(\mathbf{w}_{\text{COT}}, \mathbf{b}) \leq \text{OT}_\lambda(\mathbf{c}, \mathbf{b})$$

for $\forall \mathbf{c} \in \Delta_n$ since \mathbf{w}_{COT} minimizes this loss. This gives us the bound

$$0 \leq \text{OT}_\lambda(\mathbf{w}_{\text{COT}}, \mathbf{b}) \leq \text{OT}_\lambda(\mathbf{w}^*, \mathbf{b}).$$

Since the entropy penalized optimal transport problem does not metrize weak convergence, we require that $\lambda \rightarrow 0$.

As $\lambda \rightarrow 0$ and $n, m \rightarrow \infty$,

$$\text{OT}_\lambda(\mathbf{w}^*, \mathbf{b}) \rightarrow 0$$

since $\mathbf{w}^* \rightarrow \beta$. This implies that

$$\text{OT}_\lambda(\mathbf{w}_{\text{COT}}, \mathbf{b}) \rightarrow 0,$$

which implies that $\mathbf{w}_{\text{COT}} \rightarrow \beta$ by Corollary 6.9 in Villani (2006) since at $\lambda = 0$, $\text{OT}_\lambda = \text{OT}$.

Sinkhorn divergence. By Theorem 1 of Feydy et al. (2018), S_λ is convex in its entries, though only one entry at a time. Thus,

$$0 \leq S_\lambda(\mathbf{w}_{\text{COT}}, \mathbf{b}) \leq S_\lambda(\mathbf{c}, \mathbf{b})$$

for all $\mathbf{c} \in \Delta_n$. Thus

$$0 \leq S_\lambda(\mathbf{w}_{\text{COT}}, \mathbf{b}) \leq S_\lambda(\mathbf{w}^*, \mathbf{b}),$$

$\forall n, m$. Since $\mathbf{w}^* \rightarrow \beta$,

$$S_\lambda(\mathbf{w}^*, \mathbf{b}) \rightarrow 0$$

as the sample size goes to infinity. This implies that $S_\lambda(\mathbf{w}_{\text{COT}}, \mathbf{b}) \rightarrow 0$ and $\mathbf{w}_{\text{COT}} \rightarrow \beta$ by Theorem 1 in Feydy et al. (2018). □

The proof of Corollary 1 is immediate since $\mathbf{w}^* \rightarrow \beta$, implying that $\lim_{n \rightarrow \infty} \mathbf{w}_{\text{COT}} = \lim_{n \rightarrow \infty} \mathbf{w}^* = \beta$. This follows as a consequence of the Radon-Nikodym theorem which states that these weights mapping from α to β must be unique almost surely.

A.2 Empirical convergence

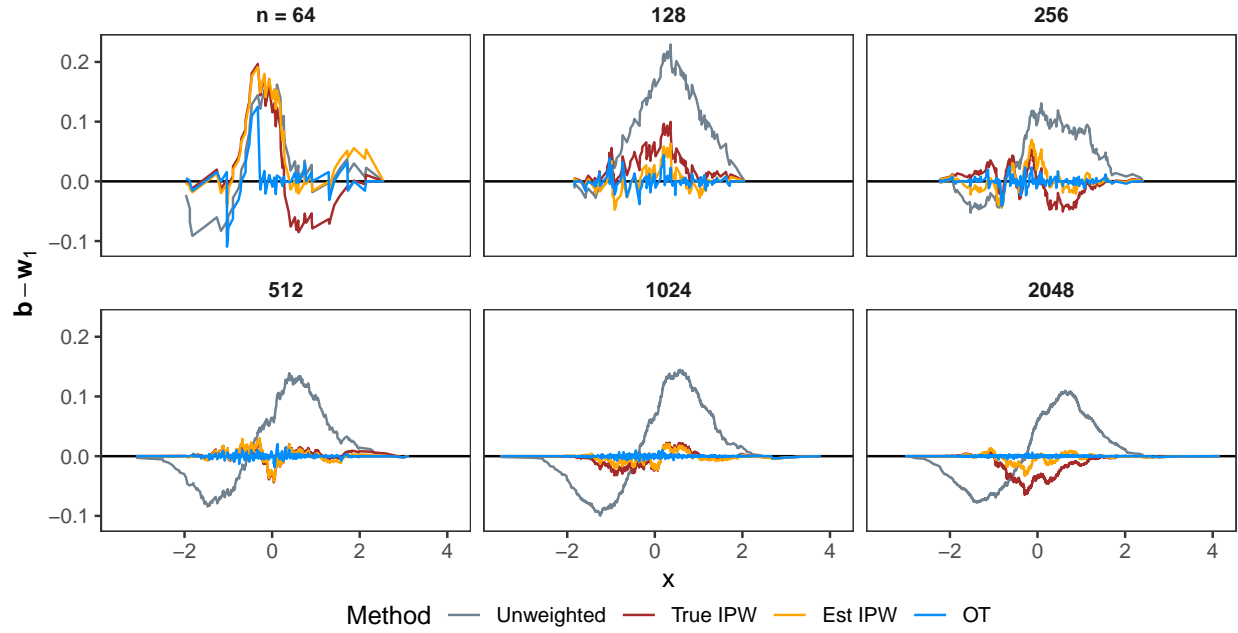
To study the convergence of our weighting estimator, we provide two simulation studies. In the first, we rely on an example discussed in Huling and Mak (2020). In the second, we use the data generating model in the high-overlap scenario of Section 5.

A.2.1 Toy example

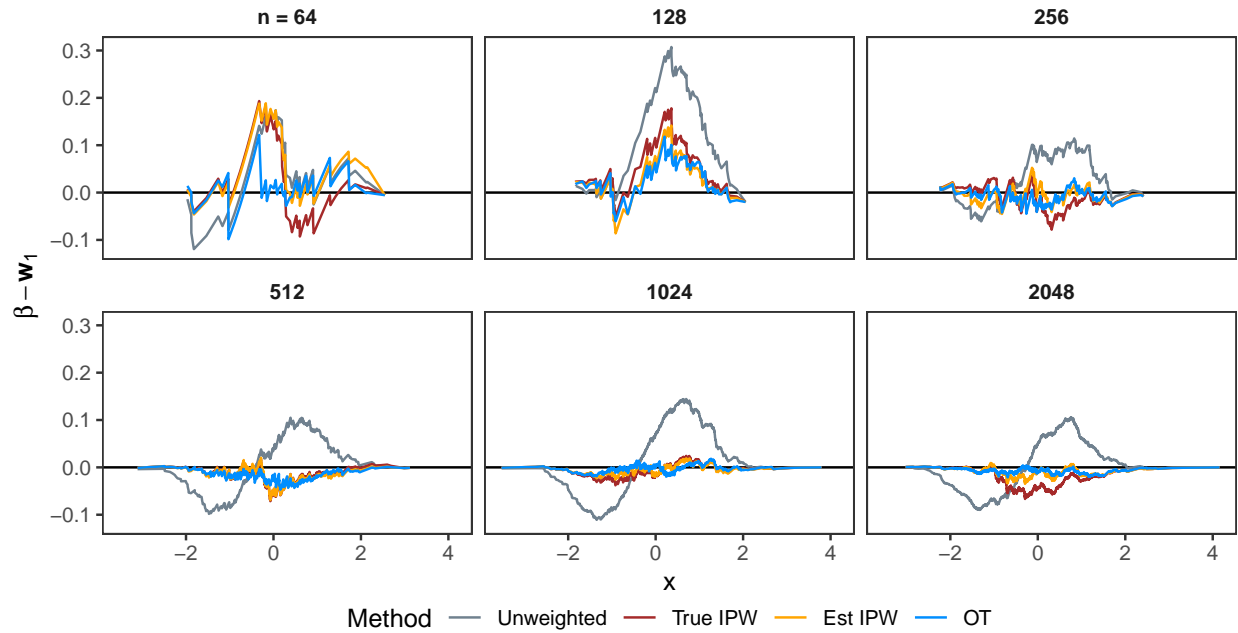
We draw a univariate covariate $X \sim \mathcal{N}(0, 1)$ and then create a treatment indicator $Z \sim \text{Bern}(p)$, with $\text{logit}(p) = -\frac{1}{3}X^3 + \frac{2}{3}X^2 + X - 1$. With this data, we then attempt to re-weight the treated group ($Z = 1$) to approximate the distribution in the full sample.

The comparator methods include the unweighted treated sample, the true propensity scores, and the

estimated propensity scores using the true model. To evaluate performance, we subtract the weighted empirical CDF of the treated, w_1 , from 1) the empirical CDF of the full sample, b , and 2) the asymptotic CDF (β) over a variety of sample sizes (Figure 9). Empirically, Causal Optimal Transport does converge to the true distribution and, at least in a univariate setting, faster than even the true model.



(a) Difference between weighted CDFs of the treated and the empirical CDF of the full sample.



(b) Difference between weighted CDFs of the treated and the asymptotic CDFs of the full sample

Figure 9: Empirical convergence of various weighted CDFs to the empirical and asymptotic CDFs

A.2.2 Convergence in the data generating model of Section 5

Causal Optimal Transport also displays favorable convergence properties in a more realistic setting. The data generating model comes from the setting in Section 5 with high-overlap between covariate distributions, and the target distribution, \mathbf{b} , in this setup is the full sample making the estimand of interest the SATE.

We then examine three measures of performance in two different scenarios. The first scenario compares the various Causal Optimal Transport methods proposed in this paper while the second compares the top performing Causal Optimal Transport method to other weighting schemes. Both scenarios evaluate the estimated weights, \mathbf{w} , at approximating 1) the target empirical distribution, \mathbf{b} , in terms of 2-Sinkhorn divergence, 2) the self-normalized propensity score, \mathbf{w}^* , in terms of the 2-Sinkhorn divergence, and 3) the difference between \mathbf{w} and \mathbf{w}^* under an L_2 norm. We present averages across 1000 replications.

For the first scenario comparing the Causal Optimal Transport methods, we can see that the Causal Optimal Transport weights using the Sinkhorn divergence better approximate both the full sample distribution and the distribution denoted by the inverse propensity score (Figure 10). Further, Figure 11 shows that while the other flavors of Causal Optimal Transport initially approximate the true inverse propensity score better under an L_2 metric, the Sinkhorn divergence quickly outperforms the other methods on average as the sample size increases.

The second scenario compares Causal Optimal Transport using Sinkhorn divergences to a variety of methods and again demonstrates the favorable performance of Causal Optimal Transport. These comparator methods are: a Probit Generalized Linear Model (GLM), the true data-generating model; Stable Balancing Weights (SBW) using the correct propensity score covariate functions; and Nearest Neighbor Matching (NNM) with replacement, which is of course equivalent to a unpenalized Causal Optimal Transport (see Section 4). For NNM, we use a cost function that is equal to $\|\cdot\|_p^p$ with $p = d/2 + 1$ to meet the conditions of Theorem 1 in Fournier and Guillin (2015) and give \sqrt{n} -convergence rates.

In Figure 12, we see that the Causal Optimal Transport weights do a better job of approximating the target distribution under the 2-Sinkhorn Divergence but that the GLM model does better at targeting the distribution implied by the true inverse propensity score under the same metric. Of note, SBW displays decaying rates convergence as the sample size increases and even performs worse than NNM.

Figure 13 displays the convergence in L_2 norm for the various methods. As we would expect, the GLM model converges fastest to the values of the true inverse propensity score. The Causal Optimal Transport weights using the Sinkhorn divergence display slightly worse rates of convergence, on average, followed by NNM. SBW again display a rate that decays with the sample size, though it does perform better than other

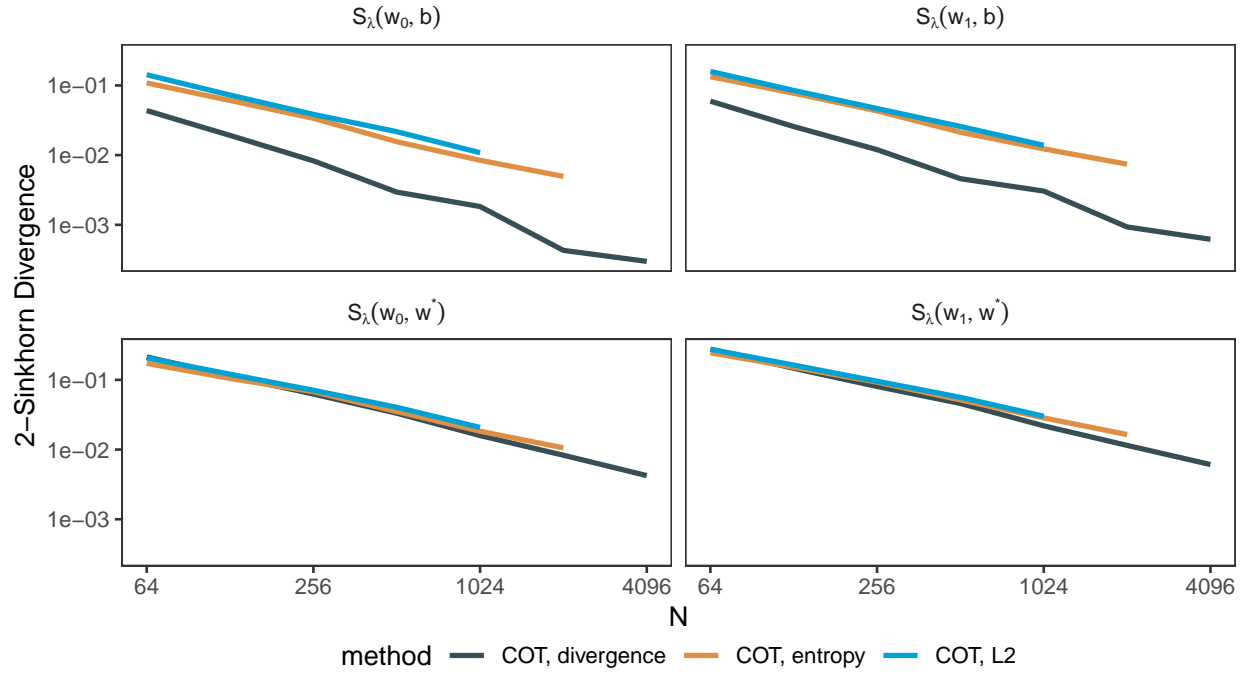


Figure 10: Convergence of the Causal Optimal Transport weights to the distributions specified by the empirical distributions (top) and the distributions specified by the true inverse propensity score/Radon-Nikodym derivatives (bottom). Lines denote means across 1000 simulations. Both axes are on the log scale.

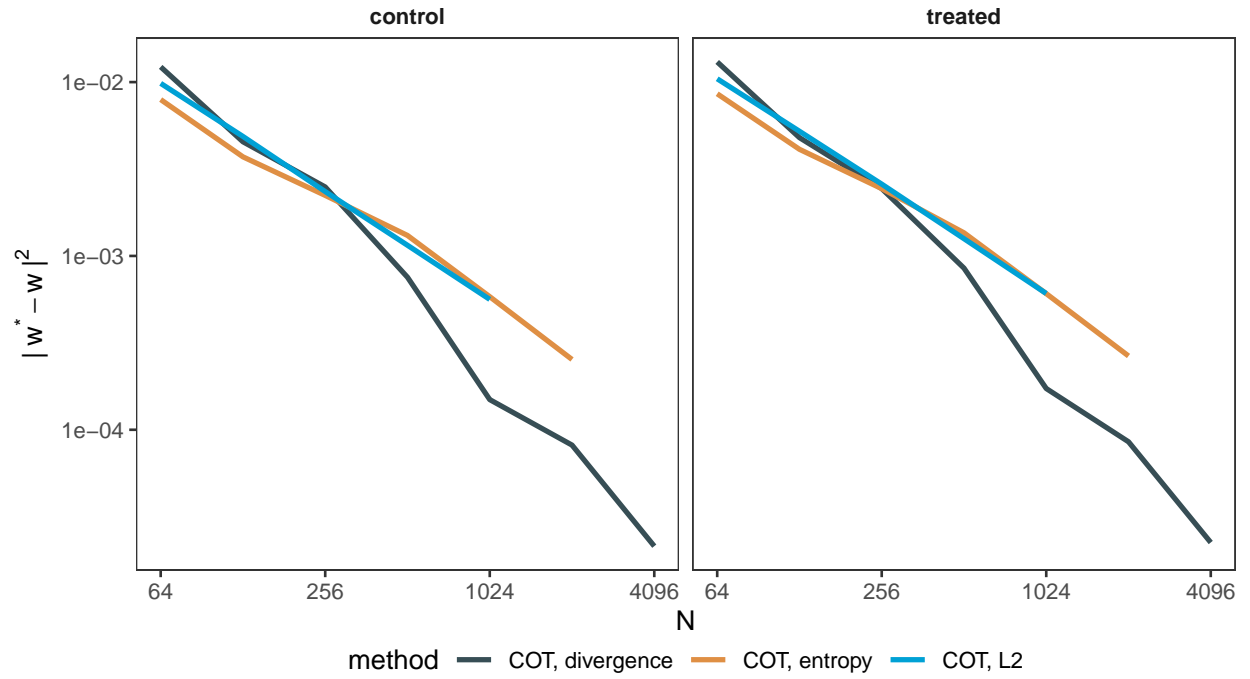


Figure 11: Convergence of the Causal Optimal Transport weights to the values of the true inverse propensity score in terms of the L_2 norm. Lines denote means across 1000 simulations. Both axes are on the log scale.

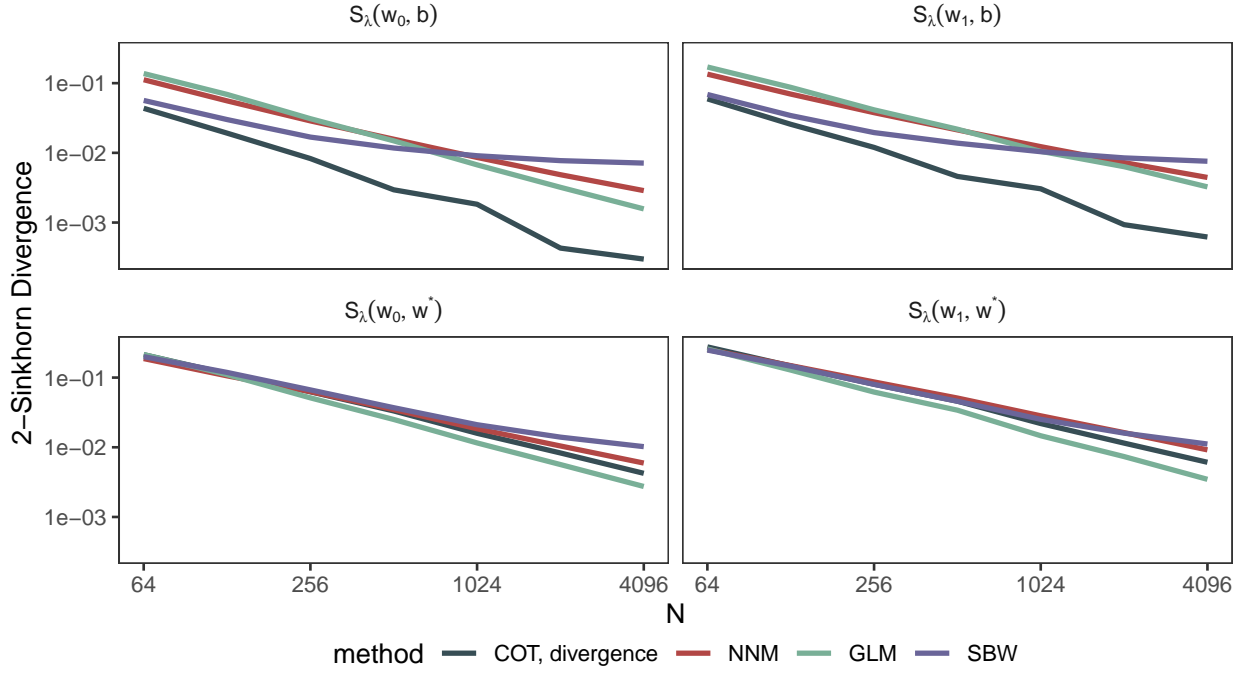


Figure 12: Convergence of the weights to the distributions specified by the empirical distributions (top) and the distributions specified by the true propensity score/Radon-Nikodym derivatives (bottom). Weights are a Causal Optimal Transport (COT), Nearest Neighbor Matching (NNM), a Probit model (GLM), and Stable Balancing Weights (SBW). Lines denote means across 1000 simulations. Both axes are on the log scale.

methods when sample sizes are small.

B Proof of Theorem 2

We now prove the speed of convergence for the Causal Optimal Transport methods.

Proof. First, \mathbf{w}^* exist under Assumptions 2 and 3 and $\mathbf{w}^* \rightarrow \beta$ by Lemma 1. Also, under Assumption 4, Theorem 1 holds and $\mathbf{w}_{\text{COT}} \rightarrow \beta$.

L₂ regularization. Theorem 1 of Blondel et al. (2018) give bounds on $\text{OT}_\lambda(\mathbf{a}, \mathbf{b})$:

$$\frac{\lambda}{2} \sum_{i,j} \left(\frac{\mathbf{a}_i}{n} + \frac{\mathbf{b}_j}{m} - \frac{1}{mn} \right)^2 \leq \text{OT}_\lambda(\mathbf{a}, \mathbf{b}) - \text{OT}(\mathbf{a}, \mathbf{b}) \leq \frac{\lambda}{2} \min\{\|\mathbf{a}\|^2, \|\mathbf{b}\|^2\}.$$

This implies that regularized problem converges at a linear rate to the unregularized problem because $\min\{\|\mathbf{a}\|^2, \|\mathbf{b}\|^2\} = \|\mathbf{b}\|^2$ because under an iid assumption $b_j = 1/m, \forall j$. Therefore,

$$\text{OT}_\lambda(\mathbf{a}, \mathbf{b}) \leq \text{OT}(\mathbf{a}, \mathbf{b}) + \frac{\lambda}{2} \|\mathbf{b}\|^2.$$

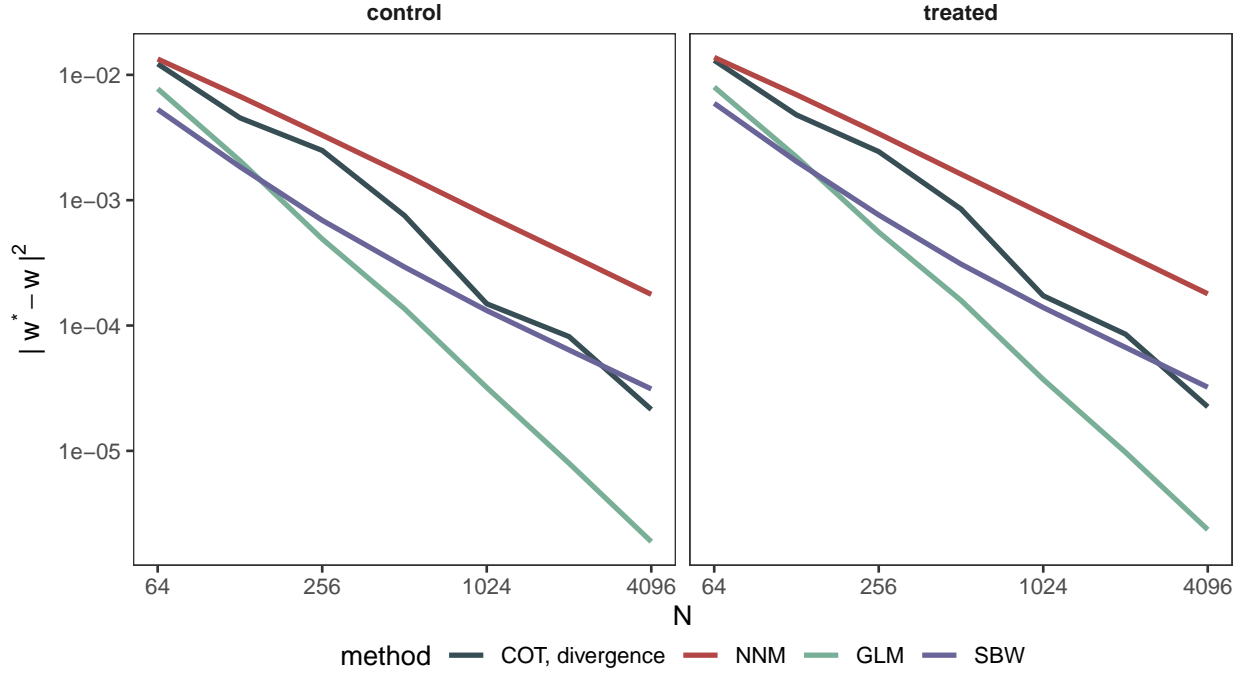


Figure 13: Convergence of the estimated weights to the values of the true inverse propensity score in terms of the L_2 norm. Weights are a Causal Optimal Transport (COT), Nearest Neighbor Matching (NNM), a Probit model (GLM), and Stable Balancing Weights (SBW). Lines denote means across 1000 simulations. Both axes are on the log scale.

Then

$$\|\mathbf{b}\|_2^2 = \sum_j \mathbf{b}_j^2 = \frac{1}{m} \rightarrow 0.$$

This also implies that

$$\lim_{n,m \rightarrow \infty} \text{OT}_\lambda(\mathbf{w}_{\text{COT}}, \mathbf{b}) = \text{OT}_\lambda(\beta, \beta) = \text{OT}(\beta, \beta)$$

since $\mathbf{w}_{\text{COT}} \rightarrow \beta$.

Further, using Theorem 1 in Fournier and Guillin (2015) we have that under Assumption 5.3,

$$\mathbb{E}\{\text{OT}(\mathbf{w}_{\text{COT}}, \mathbf{b})\} \leq \mathbb{E}\{\text{OT}(\mathbf{w}_{\text{COT}}, \beta) + \text{OT}(\mathbf{b}, \beta)\} = \mathcal{O}\left(\frac{1}{\sqrt{n}}\right).$$

Then,

$$\mathbb{E}\{\text{OT}(\mathbf{w}_{\text{COT}}, \mathbf{b}) - \text{OT}_\lambda(\beta, \beta)\} = \mathbb{E}\{\text{OT}(\mathbf{w}_{\text{COT}}, \mathbf{b})\} = \mathcal{O}\left(\frac{1}{\sqrt{n}}\right).$$

Entropy regularization. First, by convexity

$$0 \leq \text{OT}_\lambda(\mathbf{w}_{\text{COT}}, \mathbf{b}) \leq \text{OT}_\lambda(\mathbf{w}^*, \mathbf{b})$$

and

$$0 \leq \text{OT}_\lambda(\mathbf{b}, \mathbf{b}) \leq \text{OT}_\lambda(\mathbf{w}_{\text{COT}}, \mathbf{b}).$$

Also,

$$\text{OT}_\lambda(\mathbf{b}, \mathbf{b}) - \text{OT}_\lambda(\beta, \beta) \leq \text{OT}_\lambda(\mathbf{w}_{\text{COT}}, \mathbf{b}) - \text{OT}_\lambda(\beta, \beta) \leq \text{OT}_\lambda(\mathbf{w}^*, \mathbf{b}) - \text{OT}_\lambda(\beta, \beta).$$

Then with Assumptions 5.1–5.2, the conditions of either Theorem 3 of Genevay et al. (2018b) or Corollary 1 of Mena and Weed (2019) hold. This means that

$$\mathbb{E} \{ \text{OT}_\lambda(\mathbf{w}^*, \mathbf{b}) - \text{OT}_\lambda(\beta, \beta) \} = \mathcal{O} \left(\frac{1}{\sqrt{n}} \right)$$

and

$$\mathbb{E} \{ \text{OT}_\lambda(\mathbf{b}, \mathbf{b}) - \text{OT}_\lambda(\beta, \beta) \} = \mathcal{O} \left(\frac{1}{\sqrt{n}} \right).$$

Thus,

$$\mathbb{E} \{ \text{OT}_\lambda(\mathbf{w}_{\text{COT}}, \mathbf{b}) - \text{OT}_\lambda(\beta, \beta) \} = \mathcal{O} \left(\frac{1}{\sqrt{n}} \right).$$

Sinkhorn divergence. In the case of the Sinkhorn divergence, we again rely on Assumptions 5.1–5.2. We have

$$0 = S_\lambda(\mathbf{b}, \mathbf{b}) \leq S_\lambda(\mathbf{w}_{\text{COT}}, \mathbf{b}) \leq S_\lambda(\mathbf{w}^*, \mathbf{b}),$$

since the problem is convex by Theorem 1 of Feydy et al. (2018). If we add $\text{OT}_\lambda(\beta, \beta) - \text{OT}_\lambda(\beta, \beta)$ to each term and rearrange, we get

$$\begin{aligned} \frac{1}{2} \{ \text{OT}_\lambda(\mathbf{b}, \mathbf{b}) - \text{OT}_\lambda(\beta, \beta) \} &\leq \text{OT}_\lambda(\mathbf{w}_{\text{COT}}, \mathbf{b}) - \frac{1}{2} \text{OT}_\lambda(\mathbf{w}_{\text{COT}}, \mathbf{w}_{\text{COT}}) - \frac{1}{2} \text{OT}_\lambda(\beta, \beta) \\ &\leq \text{OT}_\lambda(\mathbf{w}^*, \mathbf{b}) - \frac{1}{2} \text{OT}_\lambda(\mathbf{w}^*, \mathbf{w}^*) - \frac{1}{2} \text{OT}_\lambda(\beta, \beta). \end{aligned}$$

For n large enough, the last two terms will be approximately equal to

$$\frac{1}{2} \{ \text{OT}_\lambda(\mathbf{w}_{\text{COT}}, \mathbf{b}) - \text{OT}_\lambda(\beta, \beta) \}$$

and

$$\frac{1}{2} \{ \text{OT}_\lambda(\mathbf{w}^*, \mathbf{b}) - \text{OT}_\lambda(\beta, \beta) \},$$

respectively. Therefore,

$$\begin{aligned} \frac{1}{2} \{ \text{OT}_\lambda(\mathbf{b}, \mathbf{b}) - \text{OT}_\lambda(\beta, \beta) \} &\leq \frac{1}{2} \{ \text{OT}_\lambda(\mathbf{w}_{\text{COT}}, \mathbf{b}) - \text{OT}_\lambda(\beta, \beta) \} \\ &\leq \frac{1}{2} \{ \text{OT}_\lambda(\mathbf{w}^*, \mathbf{b}) - \text{OT}_\lambda(\beta, \beta) \} \\ &\leq \text{OT}_\lambda(\mathbf{w}^*, \mathbf{b}) - \text{OT}_\lambda(\beta, \beta). \end{aligned}$$

Under Assumptions 4.1–4.2 and 5.1–5.2, Theorem 1 of Genevay et al. (2018b) or Corollary 1 of Mena and Weed (2019) hold. Thus,

$$\mathbb{E}\{ \text{OT}_\lambda(\mathbf{b}, \mathbf{b}) - \text{OT}_\lambda(\beta, \beta) \} = \mathcal{O}\left(\frac{1}{\sqrt{n}}\right)$$

and

$$\mathbb{E}\{ \text{OT}_\lambda(\mathbf{w}^*, \mathbf{b}) - \text{OT}_\lambda(\beta, \beta) \} = \mathcal{O}\left(\frac{1}{\sqrt{n}}\right).$$

Thus,

$$\mathbb{E}\{ \text{OT}_\lambda(\mathbf{w}_{\text{COT}}, \mathbf{b}) - \text{OT}_\lambda(\beta, \beta) \} = \mathcal{O}\left(\frac{1}{\sqrt{n}}\right)$$

□

C Semiparametric variance

In this section, we prove the semiparametric variance of the Causal Optimal Transport methods in Appendix C.1 and demonstrate the empirical coverage in Appendix C.2

C.1 Proof of Theorem 3

Proof. Define $e_{z,i} = \mathbb{P}(Z_i = z | X_i, S_i = 1) \mathbb{P}(S_i = 1 | X_i) / \mathbb{P}(S_i = 0 | X_i)$, or the inverse weight for the TATE. This is also the inverse of the Radon-Nikodym derivative. As a reminder, $\mu_z(X) = \mathbb{E}(Y(z) | X)$. We first decompose $\hat{\tau} - \tau$ into several residual terms:

$$\begin{aligned} \hat{\tau} - \tau &= \sum_i w_i Z_i Y_i - \sum_i w_i (1 - Z_i) Y_i - \tau \\ &= \sum_i w_i Z_i \{Y_i - \mu_1(X_i)\} - \sum_i w_i (1 - Z_i) \{Y_i - \mu_0(X_i)\} \\ &\quad + \sum_i w_i Z_i \mu_1(X_i) - \sum_i w_i (1 - Z_i) \mu_0(X_i) - \tau \\ &= \sum_i w_i Z_i \{Y_i - \mu_1(X_i)\} - \sum_i w_i (1 - Z_i) \{Y_i - \mu_0(X_i)\} \end{aligned}$$

$$\begin{aligned}
& + \sum_i w_i Z_i \mu_1(X_i) - \sum_i w_i (1 - Z_i) \mu_0(X_i) - \tau \\
& = \frac{1}{n} \sum_i \frac{Z_i}{e_{1,i}} \{Y_i - \mu_1(X_i)\} - \frac{1}{n} \sum_i \frac{1 - Z_i}{e_{0,i}} \{Y_i - \mu_0(X_i)\} \\
& \quad + \sum_i \left(w_i - \frac{1}{n \cdot e_{1,i}} \right) Z_i \{Y_i - \mu_1(X_i)\} \\
& \quad - \sum_i \left(w_i - \frac{1}{n \cdot e_{0,i}} \right) (1 - Z_i) \{Y_i - \mu_0(X_i)\} \\
& \quad + \sum_i w_i Z_i \mu_1(X_i) - \sum_i w_i (1 - Z_i) \mu_0(X_i) \\
& \quad - \frac{1}{m} \left\{ \sum_j \mu_1(X_j) - \sum_j \mu_0(X_j) \right\} \\
& \quad + \frac{1}{m} \left\{ \sum_j \mu_1(X_j) - \sum_j \mu_0(X_j) \right\} - \tau \\
& = A + B + C,
\end{aligned}$$

where

$$\begin{aligned}
A &= \frac{1}{n} \sum_i \frac{Z_i}{e_{1,i}} \{Y_i - \mu_1(X_i)\} - \frac{1}{n} \sum_i \frac{1 - Z_i}{e_{0,i}} \{Y_i - \mu_0(X_i)\} \\
& \quad + \frac{1}{m} \left\{ \sum_j \mu_1(X_j) - \sum_j \mu_0(X_j) \right\} - \tau \\
B &= \frac{1}{n} \sum_i \left(n \cdot w_i - \frac{1}{e_{1,i}} \right) Z_i \{Y_i - \mu_1(X_i)\} \\
& \quad - \frac{1}{n} \sum_i \left(n \cdot w_i - \frac{1}{e_{0,i}} \right) (1 - Z_i) \{Y_i - \mu_0(X_i)\} \\
C &= \sum_i w_i Z_i \mu_1(X_i) - \sum_i w_i (1 - Z_i) \mu_0(X_i) \\
& \quad - \frac{1}{m} \left\{ \sum_j \mu_1(X_j) - \sum_j \mu_0(X_j) \right\}.
\end{aligned}$$

The goal is to show that both $n^{1/2}B$ and $n^{1/2}C$ are $o_p(1)$. Then, since A has the form of the semiparametrically efficient score function, the result follows.

First, for B , we have that $\lim_{n \rightarrow \infty} \mathbf{w} = \lim_{n \rightarrow \infty} \mathbf{w}^*$ by Corollary 1. This also implies that $\lim_{n \rightarrow \infty} n \cdot \mathbf{w}_i = 1/e_i$ since by the Radon-Nikodym theorem, the Radon-Nikodym derivative is unique almost surely. To prove that $n^{-1/2}B$ goes to 0, it will be sufficient to prove that $\frac{\sqrt{n}}{n} \sum_i \left| \left(n \cdot w_i - \frac{1}{e_{z,i}} \right) \mathbb{I}(Z_i = z) \{Y_i - \mu_z(X_i)\} \right| \rightarrow 0$. We

then have

$$\begin{aligned} \frac{\sqrt{n}}{n} \sum_i \left| \left(n \cdot w_i - \frac{1}{e_{z,i}} \right) \mathbb{I}(Z_i = z) \{Y_i - \mu_z(X_i)\} \right| &\leq \frac{\sqrt{n}}{n} \sum_i \left| \left(n \cdot w_i - \frac{1}{e_{z,i}} \right) \mathbb{I}(Z_i = z) \right| |Y_i - \mu_z(X_i)| \\ &\leq \text{ess. sup}_i \left| \left(n \cdot w_i - \frac{1}{e_{z,i}} \right) \mathbb{I}(Z_i = z) \right| \frac{1}{\sqrt{n}} \sum_i |Y_i - \mu_z(X_i)|, \end{aligned}$$

where ess. sup is the essential supremum. The first inequality is trivial while the second inequality follows as a consequence of Hölder's inequality. For the first term, we have that $\text{ess. sup}_i \left| \left(n \cdot w_i - \frac{1}{e_{z,i}} \right) \mathbb{I}(Z_i = z) \right| \xrightarrow{\text{a.s.}} 0$ as a consequence of Corollary 1. For the second term, $\mathbb{E} |Y_i - \mu_z(X_i)| < \infty$ by assumption and

$$0 \leq \text{Var} \left(\frac{1}{\sqrt{n}} \sum_i |Y_i - \mu_z(X_i)| \right) \leq \mathbb{E} \{ \{Y_i - \mu_z(X_i)\}^2 \} \leq \mathbb{E}(Y_i^2) < \infty,$$

where the last inequality is by assumption. This implies that $\frac{1}{\sqrt{n}} \sum_i |Y_i - \mu_z(X_i)| \xrightarrow{\mathcal{L}} L$ for some random variable L . Thus, we have

$$\text{ess. sup}_i \left| \left(n \cdot w_i - \frac{1}{e_{z,i}} \right) \mathbb{I}(Z_i = z) \right| \frac{1}{\sqrt{n}} \sum_i |Y_i - \mu_z(X_i)| \xrightarrow{\mathcal{L}} 0 \cdot L = 0,$$

by Slutsky's theorem.

Second, for C , we have by assumption that $S_\lambda(\mathbf{w}, \mathbf{b}) = o_p(n^{-1/2})$. This means that the empirical distributions converge at a faster than \sqrt{n} -rate. This also implies that the empirical expectations will converge at a faster than \sqrt{n} -rate since convergence in distribution implies convergence in expectations over the distribution. Alternatively, for the basis function constraints, we have $|\mathbb{E}_{\mathbf{w}}(\mathbb{I}(Z = z)\mu_z(X)) - \mathbb{E}_{\mathbf{b}}(\mu_z(X))| \leq \sum_k \delta_k |\gamma_k| \leq \|\delta\|_2^2 \|\gamma\|_2^2$. Thus, for each value z of Z ,

$$\sqrt{n} |\mathbb{E}_{\mathbf{w}}\{\mathbb{I}(Z = z)\mu_z(X)\} - \mathbb{E}_{\mathbf{b}}(\mu_z(X))| = o_p(1).$$

Finally, with Assumption 1, we can replace Y_i with $Y_i(Z_i)$. This means that by Assumption 1 and Assumption 6.1, $\mathbb{E}(A) = 0$, which implies that $\lim_{n,m \rightarrow \infty} \mathbb{E}(\hat{\tau}) = \tau$. Thus, under Assumptions 1–6 and by the fact that A has the form of the semiparametrically efficient score function, A converges to τ at a \sqrt{n} -rate and $\hat{\tau} - \tau$ has the desired asymptotic distribution. \square

C.2 Empirical coverage of asymptotic confidence interval

The empirical coverage of the confidence interval is the focus of this subsection. We utilize the generating model from the setting in Section 5 with high-overlap between covariate distributions and the linear out-

come model (model A). The target distribution, \mathbf{b} , is the full sample, making the estimand of interest the average treatment effect. We run 1000 replications of our experiment.

Figure 14 displays results for increasing sample sizes. In the top part, Figure 14a, we see how well the methods cover the true estimate of 0 in a variety of settings. Amazingly, the Causal Optimal Transport method of Eq. (10) achieves well-calibrated confidence intervals without using an augmented estimator or mean constraints. For the methods in Eq. (9), they require either augmentation or constraints that include the correct basis functions in order to have good coverage of the truth.

In contrast, 14b shows that all methods achieve adequate coverage of their empirical expectations. In fact, the confidence intervals for the methods in Eq. (9) are conservative for their expectations when using basis function balancing but slow to converge to adequate coverage without them.

D Additional case study: the LaLonde Data

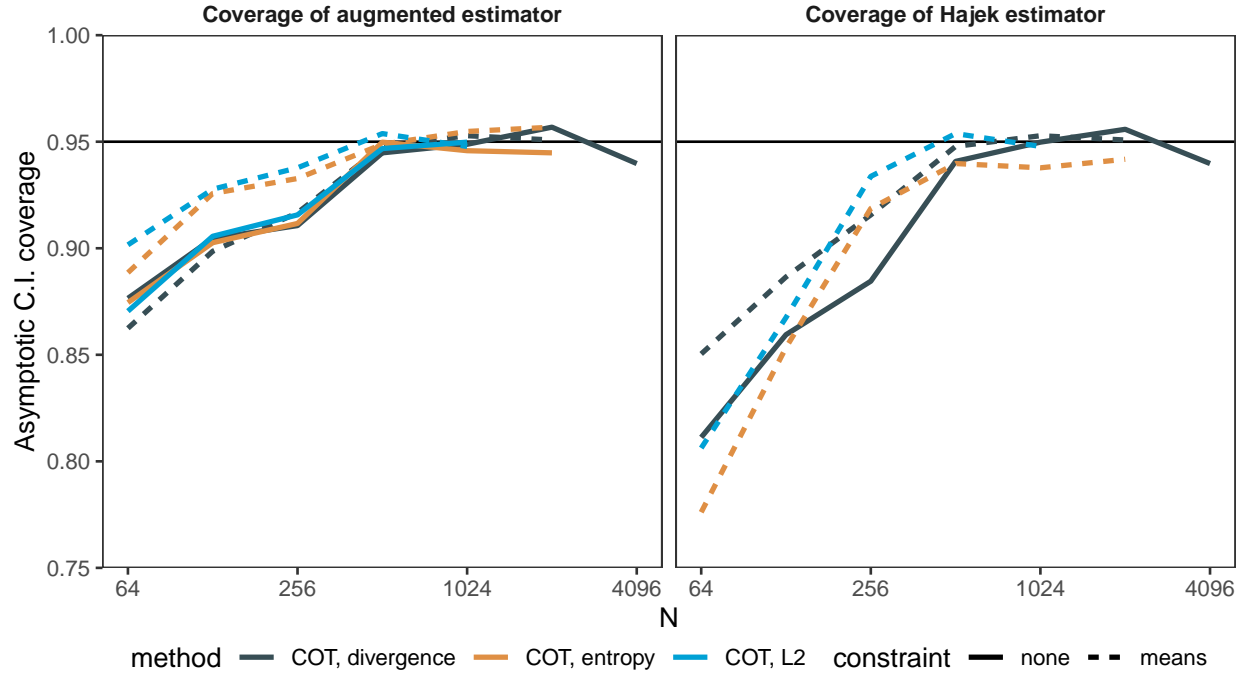
We also validate our method on the LaLonde data set (LaLonde, 1986).

D.1 The National Supported Work Demonstration program

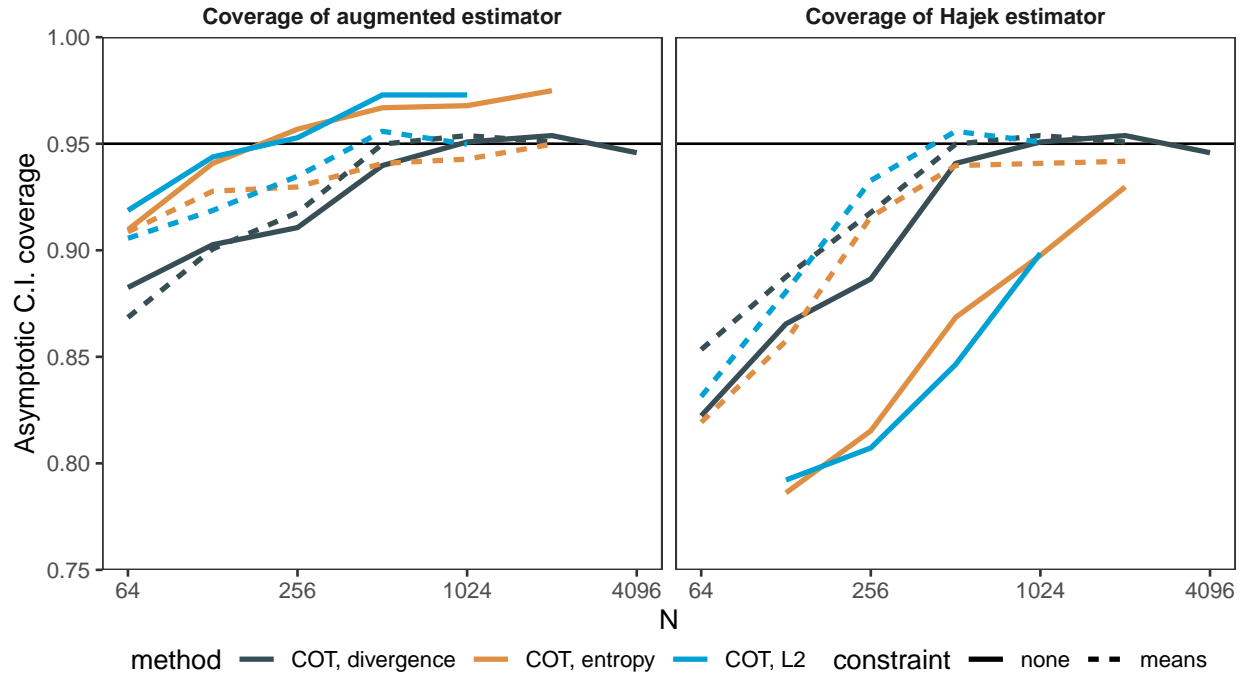
The original data come from a job training program called the National Supported Work Demonstration program (NSW) in which people were randomized to receive or not receive training from the program in the year 1976. The outcome of interest was then to look at the difference in incomes between the treatment and control groups in 1978. The original experimental estimate was a difference of \$1,794 with a confidence interval of (\$551, \$3038). The variables available in the original study include 10 pre-intervention characteristics: earnings and employment in 1974 and 1975, years of education, whether the person received a high school degree, marital status, and indicators for black or Hispanic ethnicity.

D.2 LaLonde's modification

LaLonde then proceeded to modify the original study data by removing the control group and seeing if he could recover the original treatment effect by utilizing an observational data sample taken from the Current Population Survey (CPS) with the same variables measured. This gives 185 participants from the NSM in the treated group and 15,992 non-participants from the CPS in the control group.



(a) Coverage of the true treatment effect



(b) Coverage of the average estimate treatment effect

Figure 14: Coverage of the asymptotic confidence interval for both the true effect (a) and the average estimated effect (b). The methods examined are Causal Optimal Transport (COT) with an entropy penalty (COT, entropy), COT with an L_2 penalty (COT, L2), and COT estimated using Sinkhorn Divergences (COT, divergence). Solid lines denote methods that don't balance basis functions ("none") and that balance the means of covariates ("means").

D.3 Methods

From the Causal Optimal Transport weighting methods, we include no constraints (“none”) and mean constraints (“means”). Hyperparameters were tuned with the algorithm detailed in Algorithm 1. The distance metric is an L_2 metric on the binary covariates and a Mahalanobis L_2 metric on the continuous covariates. We consider the Hajek estimator in (3), a doubly robust/augmented estimator using linear regression with linear terms of the covariates, a weighted least squares estimator, and the barycentric projection estimator of Eq. (8) utilizing an assignment matrix \mathbf{P} constructed utilizing an L_1 cost.

D.4 Design diagnostics

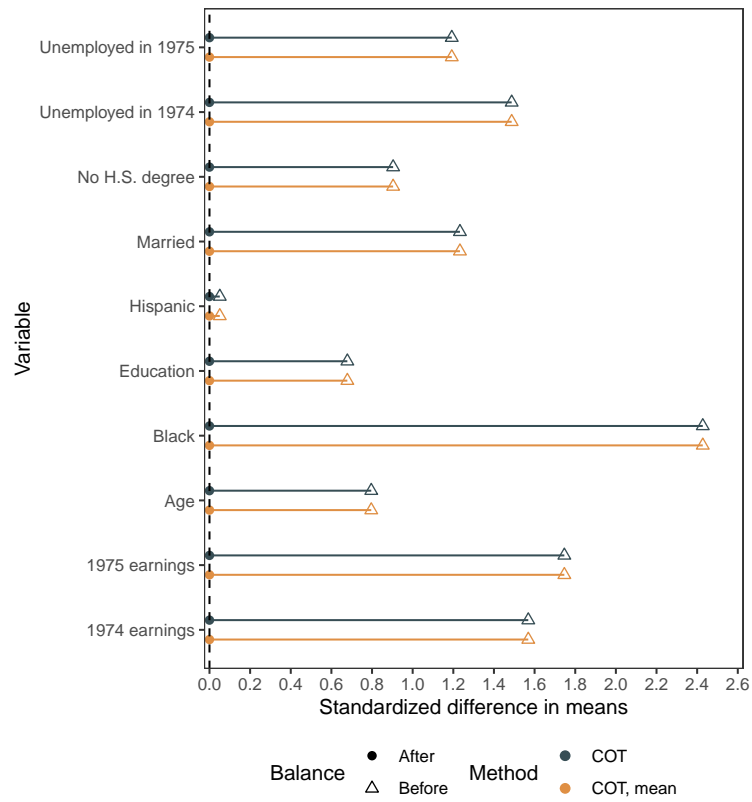
We now display the before and after weighting balance in variable means and 2-Sinkhorn divergence to give a sense of distributional balance. We can see that for all weighting methods both means and distributions are much more similar after weighting than before (Figure 15).

D.5 Results

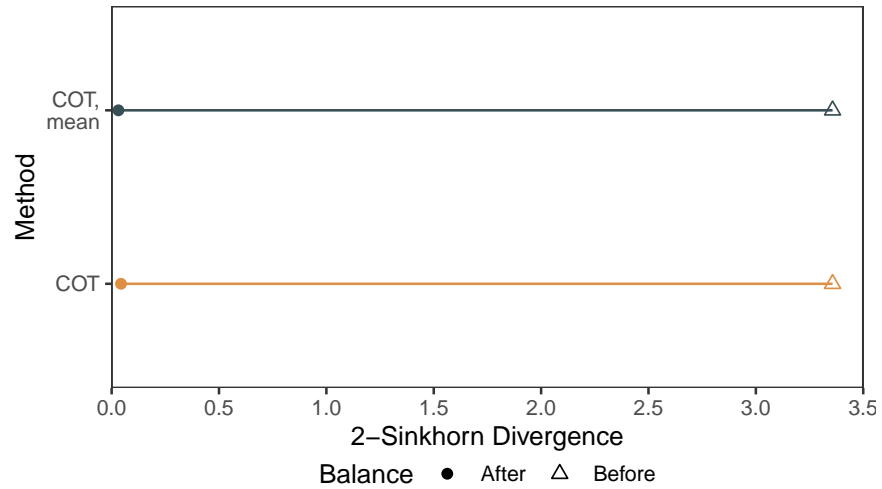
In Table 3 and Figure 16, we see that we are able to get very close to the original effects for the Hájek, Augmented, and weighted least squares approaches. The barycentric projection estimators have a notable upward bias but still have confidence intervals covering the true effect.

	Hajek	Augmented	Weighted OLS	Barycentric Projection
COT	1791 (649, 2932)	1791 (650, 2932)	1791 (418, 3164)	2435 (1287, 3583)
COT, means	1816 (675, 2957)	1816 (675, 2957)	1816 (532, 3100)	2390 (1243, 3538)

Table 3: Results for treatment effect estimation for the National Work Support demonstration treated group and the weighted set of controls from the Current Population Survey. The estimate is the difference in 1978 earnings in dollars between the two groups. Values are estimates with asymptotic 95% confidence intervals.



(a) Change in the standardized difference in means between the two groups before and after weighting



(b) Change in the 2-Sinkhorn divergence between the two groups before and after weighting

Figure 15: An examination in the change in balance before and after utilizing the optimal transport methods with the listed constraints for the LaLonde data. “COT” corresponds to no constraints and “COT, mean” corresponds to constraints on the mean balance between distributions.

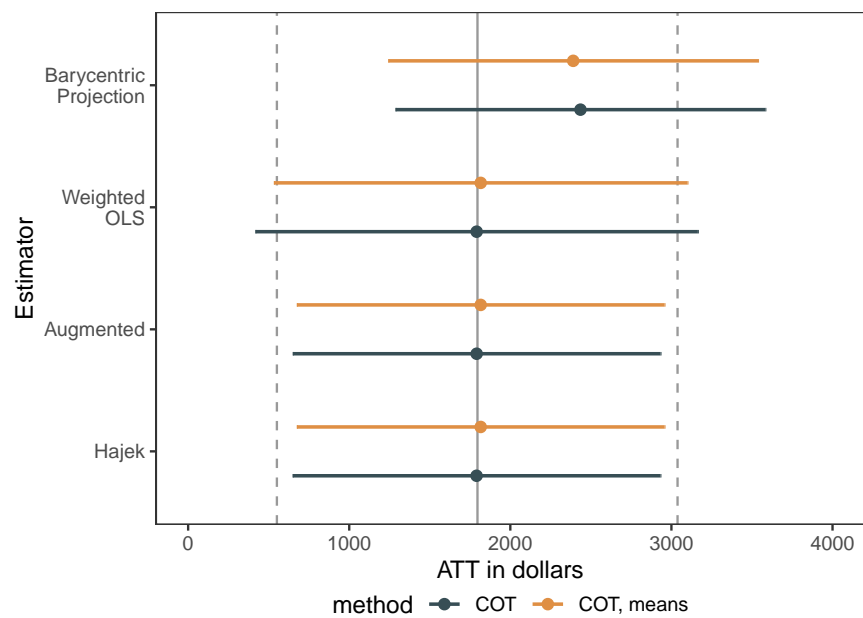


Figure 16: Results for treatment effect estimation for the National Work Support demonstration treated group and the weighted set of controls from the Current Population Survey. The estimate is the difference in 1978 earnings in dollars between the two groups targeting the average treatment effect of the treated (ATT). We see that all optimal transport methods and estimators displayed are able to get close to the original treatment effect. Note that “COT” corresponds to no constraints and “COT, mean” corresponds to constraints on the mean balance between distributions.